Sensitivities of heat-wave mortality projections: Moving towards stochastic model assumptions

Luis M. Abadie, Josué M. Polanco-Martínez

PII: S0013-9351(21)01190-7

DOI: https://doi.org/10.1016/j.envres.2021.111895

Reference: YENRS 111895

To appear in: *Environmental Research*

Received Date: 10 June 2021

Revised Date: 11 August 2021

Accepted Date: 13 August 2021

Please cite this article as: Abadie, L.M., Polanco-Martínez, Josué.M., Sensitivities of heat-wave mortality projections: Moving towards stochastic model assumptions, *Environmental Research* (2021), doi: https://doi.org/10.1016/j.envres.2021.111895.

Sensitivities of heat-wave mortality projections: moving towards stochastic model assumptions

Luis M[a] Abadie[a], Josué M. Polanco-Martínez [a,b*]

[a] Basque Centre for Climate Change (BC3), Sede Building 1, 1st floor,

Scientific Campus, University of the Basque Country UPV/EHU, 48940 Leioa, Spain.

[a] Unit of Excellence, Economic Management for Sustainability (GECOS), IME, University of Salamanca, Spain.

E-mail corresponding author*:
josue.polanco@bc3research.org

Abstract

This paper analyses the probabilistic future behaviour of heat-waves (HWs) in the city of Madrid in the twenty-first century, using maximum daily temperatures from twenty-one climate circulation models under two representative concentration pathways (RCP 8.5 & RCP 4.5). HWs are modelled considering three factors: number per annum, duration and intensity, characterised by three stochastic processes: Poisson, Gamma and truncated Gaussian, respectively. Potential correlations between these processes are also considered. The probabilistic temperature behaviour is combined with an epidemiological model with stochastic mortality risk following a generalized extreme value distribution (gev). The objective of this study is to obtain probability distributions of mortality and risk measures such as the mean value of the 5% of worst cases in the 21st century, in particular from 2025 to 2100. Estimates from stochastic models for characterising HWs and epidemiological impacts on human health can vary from one climate model to another, so relying on a single climate model can be problematic. For this reason, the calculations are carried out for 21 models and the average of the results is obtained. A sensitivity adaptation analysis is also performed. Under RCP 8.5 for 2100 for Madrid city a mean excess of 3.6ºC over the 38ºC temperature threshold is expected as the average of all models, with an expected attributable mortality of 1,614 people, but these figures may be substantially exceeded in some cases if the highest-risk cases occur.

Keywords: Heatwaves, Climate models, Stochastic diffusion modelling, Risk, Uncertainty

1. INTRODUCTION

1.1 Heat-waves

Heat-waves (HWs) are among the best-known meteorological events that regularly mark European summers (Schär et al. 2004; Vautard et al. 2013). Climate-change projections suggest that European summer heat-waves will become more frequent and severe in the 21st century (Schär et al. 2004; Meehl and Tebaldi 2004; Beniston 2004; Fischer and Schär 2010). HWs often lead to higher morbidity (illness) and mortality (death), mainly in the elderly, infants and persons with pre-existing cardiovascular and respiratory diseases (Basu and Samet 2002; Patz et al. 2005; Fischer and Schär 2010; Campbell et al. 2018). The World Health Organization (WHO, 2020) considers that heat-waves are currently and in the coming decades will continue to be one of the most natural dangerous hazards around the globe. For example, during the record-breaking HW that affected mainland Europe in summer 2003 there were

more than 70,000 deaths (Robine et al. 2008; Fischer and Schär 2010; García-Herrera et al. 2010; AghaKouchak et al. 2020). Between 1998 and 2017 HWs caused about 166,000 deaths around the world, including the 70,000 deaths in Europe in 2003 (Wallemacq 2018; AghaKouchak et al. 2020). Moreover, HWs also affect other socio-economic activities (e.g., water supply, food and livelihood security, energy and transportation, among others) and a wide range of terrestrial ecosystems (Allen et al. 2010; Smith 2011; Heres et al. 2021).

HWs typically occur when temperatures exceed thresholds set according to climatological and epidemiological criteria. Epidemiological thresholds depend on local climate conditions and may be modified by other variables such as pollution, humidity and wind. Heat-wave events therefore depend mainly on local climate and geographical conditions (Robinson 2001; Perkins and Alexander 2013; Abadie et al. 2019). However, despite their significant adverse impacts there is no single, strict definition of HWs other than as a series of consecutive hot days (Robinson 2001; Perkins and Alexander 2013; He et al. 2019). However, the World Meteorological Organization (WMO) provides a more comprehensible definition: HWs are periods of unusually hot and dry or hot and humid weather that have a subtle onset and cessation, a duration of at least two–three days, usually with a discernible impact on human and natural systems (McGregor et al., 2015). Xu et al (2016) review some definitions of HWs and find that heat-wave intensity plays a relatively more important role than duration in determining HW-related deaths. The frequency, severity and duration of HWs and the associated mortality in India between 1960 and 2009 is analysed by Mazdiyasni et al (2017) using historic data. They find statistically significant increases in heat waves in this period.

The effects of heat-waves are generally more serious in urban areas due to the urban heat island (UHI) effect (in which temperatures increase in urban areas as a result of man-made structures and activities) (Campbel et al. 2018; Abadie et al. 2019). The UHI effect has been shown to be associated with an increasing impact of HWs on populations, increasing the risk of illness and death for vulnerable residents in major cities (Tomlinson et al. 2011; Campbell et al. 2018). For this paper the city of Madrid is selected as a case study due to its size (604.3 km2), population (6.7 million in the metropolitan area) because HW events frequently occur in Madrid in summer. However, the proposed methodology could be applied to any city for which the necessary information is available. For the reasons indicated above, Madrid is frequently used to study the impacts of HW events on human health and other factors (see for example the following recent publications on the topic: Díaz et al. 2019; Follos et al. 2020; López-Bueno et al. 2020; 2021). Following the same criterion as Díaz et al. (2015; 2019), it is assumed that there is a HW in Madrid if the critical temperature of 35ºC is exceeded on one or more consecutive days. Note that according to Díaz et al. (2019) there is a different threshold for each city, depending on its different geographical patterns.

1.2 Use of stochastic diffusion models

There are various ways to analyse HWs using stochastic models. These models incorporate uncertainty into projections, enabling probability distributions to be obtained for certain future times, from which expected values and certain statistics such as volatility and percentiles can be drawn. Stochastic models for HWs can be divided into two groups depending on whether they are based on time series or on extreme values:

1.2.1 Based on time series analysis

In this approach, time series parameters are estimated as in Macchiato et al. (1993) and Kyselý (2010). There is usually a deterministic part that includes seasonal effects and the trend and a stochastic part that can be modelled as an autoregressive process of order one AR(1). The parameters of the stochastic part include the mean, the volatility and the first order autocorrelation coefficient. This stochastic part is a mean-reverting model estimated using time series of daily maximum air temperatures. When this type of model is used, low temperatures and both affect the calculations. This class of stochastic models

can be used with historical observational data, with future simulated data through regionalized climate models, and even with past climate simulations. After the parameters (deterministic and stochastic) have been calculated a number of paths can be simulated and the definition of a heat-wave applied to obtain HW behaviour (number, duration and intensity).

1.2.2 Extreme Value Theory

In this approach the models proposed are close to the techniques of Extreme Value Theory (EVT), e.g. the well-known peak-over-threshold model (POT). In this class of model, HW information is first extracted from the time series (historic or projections (future)) and fitted to a model with the frequency, intensity and duration of an HW as in Furrer el al. (2010) and Abadie et al. (2019). The parameters can vary over time according to historical or future data. After the parameters have been calculated correlated values at a time t can be simulated and distributions obtained with parameters such as the mean, median, percentiles and worst cases.

1.3 General choices to be made for HW projections

The objective of this study is not only to determine figures for expected mortality due to HWs but also to obtain distributions of mortality and risk measures such as the mean value of the 5% of worst cases in the distribution (ES (95%)). The scenarios selected are RCP 4.5 and RCP 8.5 in the 21st century, and more specifically from 2025 to 2100. The calculations are made for 21 models with the average of their parameters, expected values and risk measures being obtained.

Mortality risk projections will be calculated using an epidemiological model and considering the uncertainty of mortality risk (MR) in that model. The possibility of acclimatisation by absorbing the impact of half the expected excess temperature is also considered as a sensitivity analysis.

The rest of the paper is organized as follows: Section 2 describes the materials and methods used. Section 3 shows the results for HWs and the associated mortality risk and discusses the main results. Section 4 presents the main conclusions.

2. MATERIALS and METHODS

2.1 Stochastic diffusion models

Some studies on HWs that use stochastic models are cited below in the following lines. For example, Furrer et al. (2010) propose a stochastic model with a Poisson process for the number of HWs per year, a geometric distribution for duration and a Generalized Pareto (GP) distribution for excess temperature. Their model is calibrated with historical data from Phoenix, Arizona (US), Fort Collins, Colorado (US) and Paris (France). Some years later, Abadie et al. (2019) calibrate a stochastic diffusion model to characterize statistics of extreme events using future data from a climate model. The three-factor model proposed uses a Poisson process for the number of heat waves, a Gamma process for the mean duration and a truncated Gaussian process for mean excess temperature, where potential correlations between the three processes are considered in building the three-variate model. On the other hand, Coles et al. (1994) proposed and used some models based on the bivariate extreme value theory.

When modelling future heat waves, it is important to take into account the non-stationary nature of climate change. According to Kharin et al. (2007), the uncertainty in modelling the climate strongly affects the values taken as extremes. Moreover, Brown et al. (2008) analyse changes in extreme daily temperatures since 1950 using an extreme value distribution with time-varying parameters. In their model events are assumed to occur according to a Poisson process, and the excesses above the threshold are assumed to follow a Generalized Pareto distribution.

In this paper two stochastic models are used, the first for temperature and the second an epidemiological model.

2.1.1 Temperature model

The critical temperature was calculated using the methodology of Diaz et al. (2015) with daily maximum daily temperatures from 2010 to 2018 in the meteorological station el Retiro of Madrid City (AEMET, 2021) and daily natural mortality of Madrid city for the same period, that information was provided by the Spanish National Institute of Statistics (INE, 2021), a methodology description is shown in Appendix A.1. A value of 38ºC was calculated for this critical temperature above which there is a significant increase in daily mortality in Madrid city.

We follow the temperature stochastic model in Abadie, et al. (2019), a brief description of which is provided in Appendix A.2. This model takes into account three stochastic characteristics of HWs: (1) the number of HWs in a given year; (2) their duration in days; and (3) their intensity measured by their exceedance of the critical temperature of 38ºC. Two correlations are also included in the model: (1) an expected negative correlation between the number of HWs per year and their durations (because a longer duration is usually associated with a lower number of HWs); and (2) the correlation between the duration of HWs and their temperature exceedances, with higher temperature exceedance expected for longer-lasting HWs. The three HW characteristics in the model (number, duration and intensity) have expected values that change over time according with exponential parameters. Table 1 shows the parameters to be calibrated for each of the 21 temperature models. These parameters are calibrated using nonlinear least squares for each model. In this study, all possible HWs in the year are used and not only those in the summer.

Table 1: Temperature model parameters

Parameter	Units	Description
$\lambda(t)$	(-)	Number of HWs in year t
α	(y^{-1})	Exponential parameter of number of HWs $\lambda(0)$
dur(t)	(days)	HW duration
γ	(y^{-1})	Exponential parameter of HW duration $d(0)$
$g(t)$	(°C)	Temperature exceedance above 38ºC
β	(y^{-1})	Exponential parameter of temperature excess $g(0)$
σ_E	(°C)	Volatility of temperature excess
$\rho_{1,2}$	(-)	Correlation of number of HWs and duration
$\rho_{2,3}$	(-)	Correlation of duration and temperature excess
σ_D	(days)	Volatility of duration

2.1.2 Epidemiological model

A model for mortality risk projections is used as per epidemiological Equation (1), where mortality for a HW is proportional to the product of HW days and excess temperature as in Diaz et al. (2015). In this epidemiological model, HW-related mortality is also proportional to the specific mortality risk for Madrid city and to the background daily mortality. Formality ratios are as defined below (Diaz et al. 2015).

$$M_t = MR \times B \times \sum_{i=0}^{k_t} (\Delta T_i \times N_i) \quad (1)$$

Where:

$B = 74.26$ is the background daily mortality rate for death from natural causes during HW days calculated using the mortality data for Madrid city (from 2010 to 2018) and the critical temperature of 38ºC.

ΔT_i is the excess temperature over the threshold ($T_{max} - T_{crit}$) for HW *i* in year *t*.

N_i is the duration of HW *i* in year *t*.

k_t is the number of HWs in year *t*.

k_t, N_i and ΔT_i correspond to the three variables of the stochastic temperature models (number, duration and excess temperature of HWs). There is also a fourth stochastic variable in the form of the mortality risk (MR). This variable is modelled as a generalised extreme value distribution (gev) as shown in Appendix A.3.

The relative risk was calculated using the cited data obtain a value of 1.05 with a 95% confidence interval (CI) (1.02, 1.08). Then the mortality risk (MR) in Madrid is 4.76% within a 95% confidence interval (CI) (1.96%, 7.41%). Using these percentiles, the GEV parameters are calculated as $\mu = 4.2828, \sigma = 1.4379$ and $\xi = -0.3158$. These calculations are applied for each Monte Carlo simulation using the four stochastic variables and a distribution of annual mortality is obtained for each model.

2.2 Assumptions explored and climate data

In this study, three indicators are calculated. The first is the mean (or expected value) and the other two are risk measures: the Value at Risk VaR (95%) is the 95th percentile and the Expected Shortfall (ES) (95%) is the average of 5% worst cases. Technically ES (95%) is considered a better measure of risk than VaR (95%) since it provides more information about the tail of the distribution with more harmful values. Here, risk is considered to mean that something worse than expected could happen.

Daily maximum near-surface air temperatures (T_{max}) for the city of Madrid (central grid) and for the study period of 2006-2100 are drawn from NASA Earth Exchange Global Daily Downscaled Projections (NEX-GDDP) (freely available at https://www.nccs.nasa.gov/services/data-collections/land-based-products/nex-gddp). The NEX-GDDP dataset comprises downscaled climate scenarios for the globe, derived from General Circulation Model (GCM) runs conducted under the Coupled Model Intercomparison Project Phase 5 (CMIP5), which includes projections for RCP 4.5 and RCP 8.5 from 21 models and scenarios for which daily scenarios were produced and distributed under the Coupled Model Intercomparison Project Phase 5 (CMIP5) (Thrasher et al. 2012; NEX-GDDP 2021). As can be seen in Table 2, the effect of bias correction is quite limited.

Table 2: Effects of the bias correction.

No.	Model	V1	V2
1	ACCESS1-0	-0.7765	1.0010
2	BNU-ESM	-0.8479	1.0043
3	CCSM4	-0.6975	0.9972
4	CESM1(BGC)	-0.7127	0.9978
5	CNRM-CM5	-0.7393	0.9989
6	CSIRO-Mk3.6.0	-0.8190	1.0032
7	CanESM2	-0.9059	1.0078
8	GFDL-CM3	-0.8149	1.0058
9	GFDL-ESM2G	-0.8825	1.0059
10	GFDL-ESM2M	-0.8956	1.0065
11	IPSL-CMSA-LR	-0.8487	1.0047
12	IPSL-CM5A-MR	-0.7604	1.0005
13	MIROC-ESM	-0.8790	1.0061
14	MIROC-ESM-CHEM	-0.8709	1.0055
15	MIROC5	-0.7495	0.9995
16	MPI-ESM-LR	-0.7917	1.0016
17	MPI-ESM-MR	-0.7947	1.0017
18	MRI-CGCM3	-0.6545	0.9948
19	NorESM1-M	-0.8471	1.0045
20	bbc-csm1-1	-0.8550	1.0049
21	inmcm4	-0.8069	1.0030

A time-frame (2025 vs 2100) is used with uncertainty in the epidemiological model (MR) modelled using a generalised extreme value distribution and the impact of acclimatisation being explored in the form of a sensitivity analysis.

3. RESULTS and DISCUSSION

3.1 Parameter estimation

Figure 1 shows the number of HWs per year, their duration and their expected values under RCP 8.5, using climate model 1 (ACCESS1-0 in Table 2). This Figure shows a substantial increase in the expected duration of HWs, which is especially conspicuous from the 2040s onwards. This result is consistent with those in Abadie et al. (2019), Chapman et al. (2019) and Perkins-Kirkpatrick and Lewis (2020). However, the trend in the number of HWs is not so clear, due to the increase in their duration over time.

Figure 2 shows the expected mean excess temperature in the case of HWs under RCP 8.5 and RCP 4.5 scenarios in climate model 1 (ACCESS1-0 in Table 2). This figure shows a faster increase in excess temperature in scenario RCP 8.5. The gap between the expected mean excess temperatures for the two scenarios widens rapidly over the years.

Figures 1 and 2 are generated using the model data and the parameters calculated. Other figures can be generated with data from other climate models and their estimated parameters, as shown in Tables A1 and A2 in the Appendix A.2.

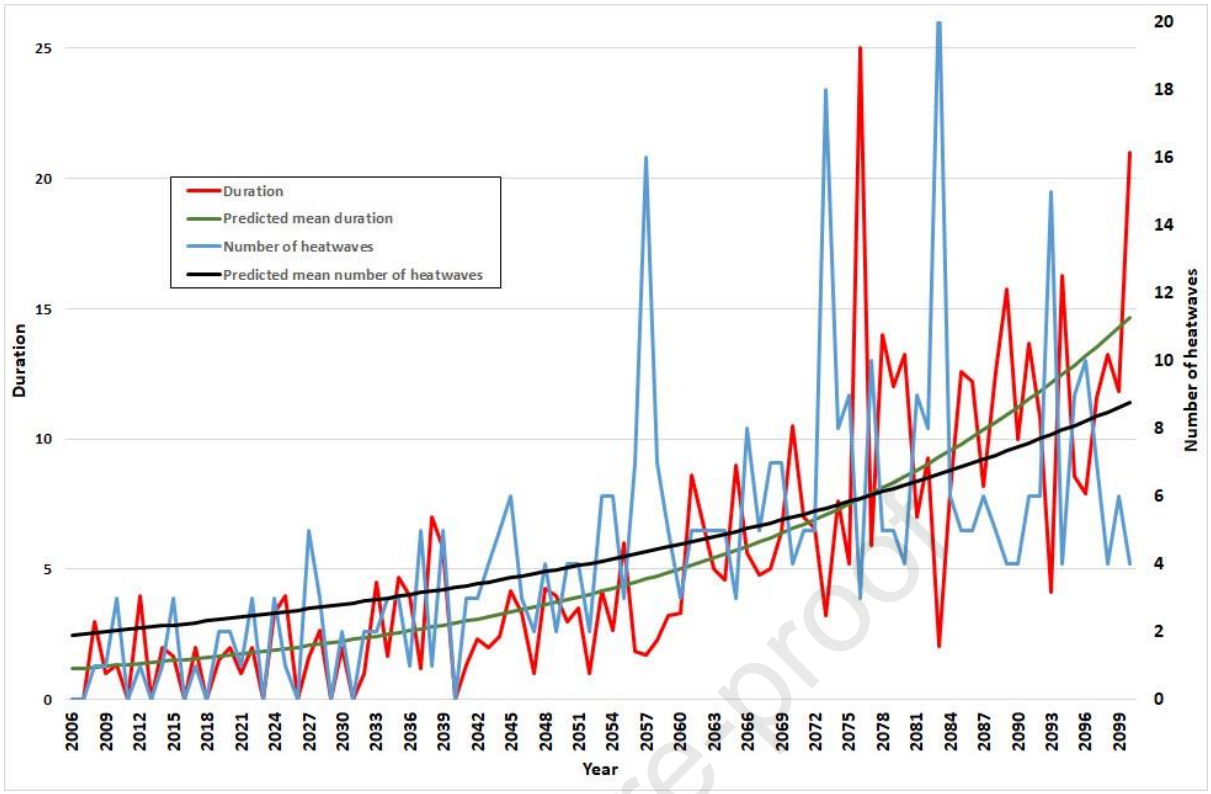

Fig 1. Evolution of HW characteristics per year (number of HWs per year and mean HW duration) as obtained from climate model 1 (see Table 2) and evolution of expected values from the fitted stochastic model under RCP 8.5.

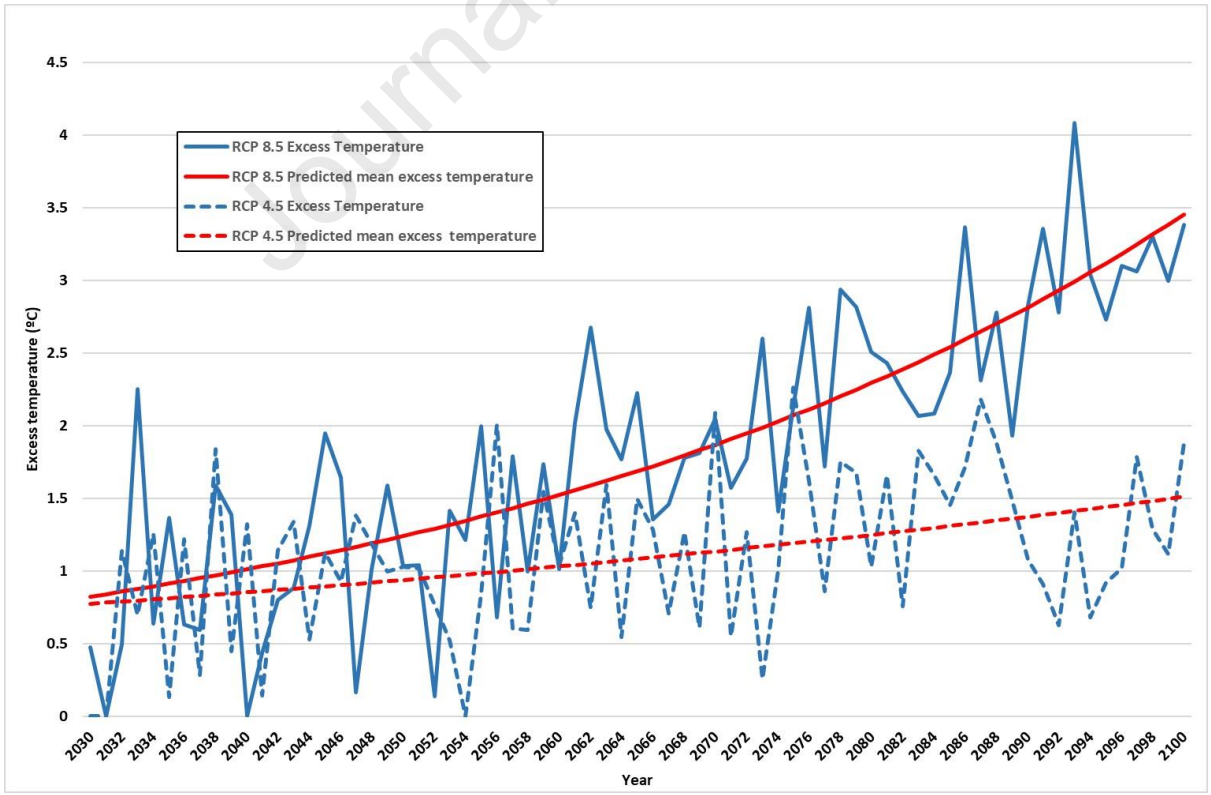

Fig 2. Evolution of mean excess temperature on HW days as obtained for climate model 1and expected values from the fitted stochastic model under RCP 4.5 and RCP 8.5.

Table 3. Model parameters for climate model 1 (ACCESS1-0).

Parameters	RCP 4.5	RCP 8.5
λ(0)	1.3919	1.9057
α	0.0153	0.0162
dur(0)	1.7678	1.1776
γ	0.0117	0.0268
temp(0)	0.6175	0.5043
β	0.0095	0.0205
σ_E	0.5458	0.5594
$\rho_{1,2}$	0.3149	0.2031
$\rho_{2,3}$	0.5851	0.3945
σ_D	1.9506	3.0525

Table 3 shows the estimated parameters for climate model 1 (ACCESS1-0) under RCP 4.5 and RCP 8.5. Table 3 shows the exponential increase in the number of HWs per year, their duration and their associated temperature excess above 38ºC. Table 3 also shows the differences in the correlations calculated ($\rho_{1,2}$ and $\rho_{2,3}$) under the two scenarios.

Tables A.1 and A.2 in Appendix A.2 presents these parameters for the 21 climate models under the RCP 4.5 and RCP 8.5 scenarios. With these values it is possible to generate figures similar to Figures 1 and 2 for climate model 1. The means are shown in Table 4. Note that these values are for a non-adaptation case. The means of the models in the RCP 4.5 and RCP 8.5 cases also show significant increases in the number, duration and excess temperature of HWs.

Table 4. Mean of stochastic model parameters.

Parameters	RCP 4.5	RCP 8.5
λ(0)	1.6212	1.9665
α	0.0134	0.0175
dur(0)	1.3089	1.0378
γ	0.0120	0.0266
temp(0)	0.5505	0.4723
β	0.0103	0.0217
σ_E	0.5953	0.5925
$\rho_{1,2}$	0.4298	0.3217
$\rho_{2,3}$	0.6448	0.5049
σ_D	1.6805	3.2623

Table 5 shows the mean of the expected values using the 21 climate models. The expected increase in all three factors (number, duration and intensity of HWs) can be seen. The mean in 2100 for expected HW duration is about triple in the RCP 8.5 scenario, with the number of HWs being 60% more. The expected excess temperature by 2100 is 3.56ºC in the RCP 8.5 scenario, which is significantly higher than the 1.48ºC that appears in the RCP 4.5 scenario. The differences between the two scenarios become significant in the mid-21st century: closest values are obtained for 2025.

Table 5. Mean of expected values using the 21 climate models.

Expected mean values	RCP 4.5	RCP 8.5
λ(t) 2025	2.06	2.60
λ(t) 2050	2.83	3.82
λ(t) 2075	3.93	5.74
λ(t) 2100	5.50	8.82
dur(t) 2025	1.63	1.65
dur(t) 2050	2.20	3.11
dur(t) 2075	2.99	6.11
dur(t) 2100	4.10	12.69
temp(t) 2025	0.67	0.70
temp(t) 2050	0.86	1.20
temp(t) 2075	1.12	2.06
temp(t) 2100	1.48	3.56

For the RCP 8.5 case the mean of the 21 climate models for 2050 in Madrid under RCP 8.5 is expected to be 3.8 HWs lasting 3.1 days, with an expected excess temperature above 38ºC of 1.2º. For the RCP 4.5 case the figure expected for 2050 is a mean of 2.8 HWs lasting 2.2 days, with an excess temperature of 0.9ºC. The gap between the excess temperatures in the two models widens significantly in the second half of the 21st century.

The figures in Tables A.1 and A.2 with the differences between models highlight the problem of relying on a single model compared to using the mean of various models as in Tables 4 and 5. One model can give significantly different results from another. Some models can generate extreme values above or below the average. If all models are equally likely, the use of such extreme values can generate results that range from alarming to non-worrisome. Note that this paper does not assume that one climate model is better or worse than another. Therefore, if only one climate model is used there is a risk in choosing it.

3.2 Stochastic projections

Figure 3 shows the distribution of the excess temperature in climate model 1 for the year 2100 under the RCP 8.5 scenario. It shows that some extreme excess temperature values are above the expected value of 3.45 ºC (see Table A.2.a for this climate model). Those extreme values are of great importance for prevention and adaptation policies because of the negative effects when these situations, which are unlikely but possible, actually happen.

Figure 4 shows the distribution of mortality in Madrid for 2100 under RCP 8.5 for climate model 1. This distribution was obtained by applying the epidemiological stochastic model to the stochastic temperature model using Equation 1. As can be seen, the expected value is 1,626 but in 5% of cases it may be more than 3,547, with the mean of the 5% of worst cases being 4,414 (see Table 7). All the expected mortality and risk values for all the models under the RCP 4.5 scenario are in Table 6. Table 7 shows the equivalent values for RCP 8.5. The mean of 21 models in Madrid for 2100 under RCP 8.5 shows an expected mortality of 1,614 with 5% of cases in which mortality is above 3,609 cases and the mean of the 5% of worst cases being 4,530 (see Table 7).

Tables 6 and 7 show the related expected mortality and risk values under RCP 4.5 and RCP 8.5, respectively.

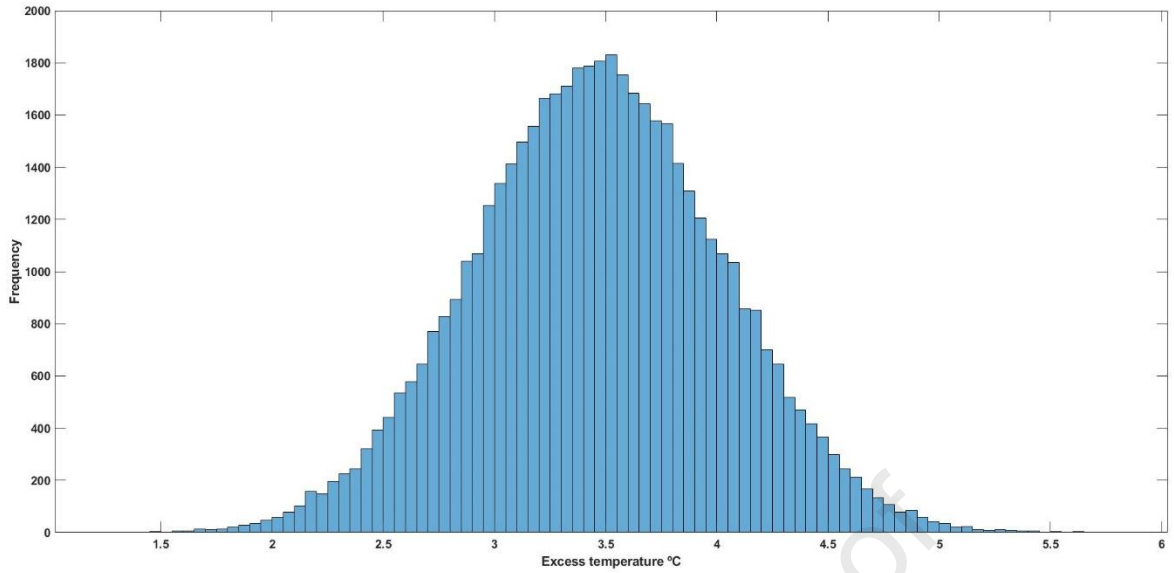

Fig 3. Histogram from Monte Carlo projections of climate model 1 of temperature exceedances in 2100 under RCP 8.5.

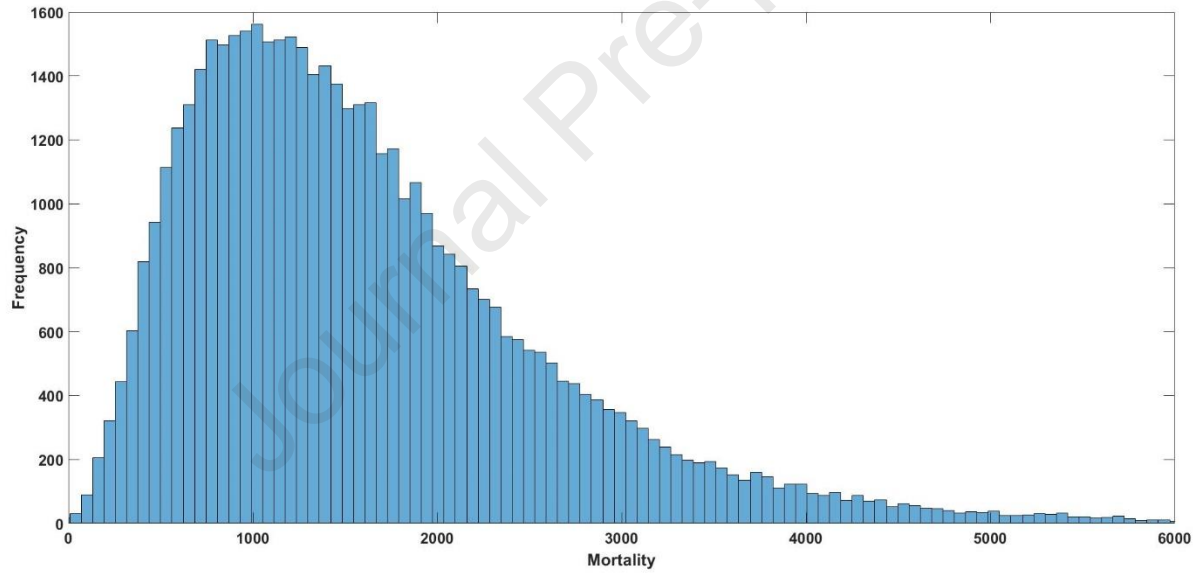

Fig 4. Histogram of climate model 1 from Monte Carlo of mortality projections for the 2100 climate and under RCP 8.5.

3.3 Analysis of sources of variation

Figure 5 shows the trends over time of the three risk measures. Expected value using a financial/economic type approach is not really a risk measure, since in such approaches the risk is the possibility of worst cases. The 95th percentile (or Value at Risk VaR(95%) can be used to establish the frontier where the worst cases begin but it does not inform about the shape of the distribution tail. The mean of the 5% worst cases, i.e. the Expected Shortfall ES(95%), is therefore considered a better measure of risk. Figures similar to Figure 5 for all other climate models can be obtained using the data from Table 6 for RCP 4.5 and that from Table 7 for RCP 8.5.

Table 6: Results for Madrid under the RCP 4.5 scenario, without adaptation.

	2025			2050			2075			2100		
	Expected	VaR(95%)	ES(95%)	Expected	VaR(95%)	ES(95%)	Expected	VaR(95%)	ES(95%)	Expected	VaR(95%)	ES(95%)
ACCESS1-0	15	70	126	34	135	212	79	264	383	187	529	730
BNU-ESM	9	46	87	19	80	134	39	137	212	78	241	340
CCSM4	17	78	137	29	115	187	47	173	267	78	258	381
CESM1(BGC)	13	62	117	24	104	174	47	174	269	91	295	421
CNRM-CM5	3	19	55	6	34	77	12	59	112	25	106	179
CSIRO-Mk3.6.0	20	90	159	50	187	289	132	402	575	351	900	1,196
CanESM2	21	82	129	48	154	226	109	306	414	250	619	803
GFDL-CM3	59	260	430	156	532	779	408	1,149	1,547	1,087	2,600	3,346
GFDL-ESM2G	12	55	101	15	69	122	20	86	145	27	110	181
GFDL-ESM2M	9	53	114	17	84	159	32	138	232	61	229	354
IPSL-CMSA-LR	4	30	79	14	72	141	48	185	291	167	492	686
IPSL-CM5A-MR	11	74	173	25	134	268	53	240	418	120	456	701
MIROC-ESM	20	81	135	49	166	249	125	348	488	322	782	1,024
MIROC-ESM-CHEM	31	115	181	75	232	333	183	477	638	459	1,050	1,338
MIROC5	11	56	107	21	95	164	41	163	253	85	289	429
MPI-ESM-LR	4	31	71	13	72	133	39	164	266	118	391	577
MPI-ESM-MR	6	31	75	15	68	124	42	153	237	128	375	522
MRI-CGCM3	2	16	56	5	34	84	14	70	134	38	151	247
NorESM1-M	19	85	144	38	140	219	73	234	339	142	405	552
bbc-csm1-1	7	38	88	12	64	120	25	109	190	53	191	294
inmcm4	1	7	28	2	15	42	4	29	62	10	55	106
NASA	14	66	123	32	123	202	75	241	356	185	501	686

Table 7: Results for Madrid under the RCP 8.5 scenario, without adaptation.

	2025			2050			2075			2100		
	Expected	VaR(95%)	ES(95%)	Expected	VaR(95%)	ES(95%)	Expected	VaR(95%)	ES(95%)	Expected	VaR(95%)	ES(95%)
ACCESS1-0	19	95	194	79	290	445	348	935	1,257	1,626	3,547	4,414
BNU-ESM	19	94	253	69	302	547	267	878	1,326	1,082	2,747	3,631
CCSM4	25	113	200	77	273	410	255	714	984	869	2,015	2,562
CESM1(BGC)	20	85	150	62	211	313	205	545	740	689	1,552	1,967
CNRM-CM5	1	14	40	10	52	100	59	212	322	357	943	1,253
CSIRO-Mk3.6.0	26	123	269	95	364	573	414	1,178	1,614	1,941	4,339	5,438
CanESM2	42	199	366	153	530	798	577	1,539	2,052	2,265	4,992	6,228
GFDL-CM3	55	296	616	262	1,027	1,634	1,076	3,100	4,236	4,467	10,172	12,716
GFDL-ESM2G	7	41	100	33	135	230	166	485	683	914	2,082	2,654
GFDL-ESM2M	14	79	156	53	208	329	202	582	811	773	1,790	2,298
IPSL-CMSA-LR	14	83	216	64	278	489	323	1,000	1,437	1,805	4,326	5,576
IPSL-CM5A-MR	14	87	250	57	292	655	337	1,246	1,920	2,585	6,064	7,758
MIROC-ESM	18	95	248	84	366	626	535	1,431	1,918	3,979	8,015	9,639
MIROC-ESM-CHEM	44	204	363	176	578	838	777	1,908	2,469	3,626	7,460	9,020
MIROC5	13	77	170	48	204	340	191	591	844	775	1,884	2,477
MPI-ESM-LR	15	90	241	67	288	502	340	1,023	1,413	1,919	4,326	5,457
MPI-ESM-MR	10	36	154	47	206	376	290	818	1,140	1,955	4,094	5,028
MRI-CGCM3	2	24	78	14	76	148	83	278	414	520	1,279	1,656
NorESM1-M	21	89	157	68	224	327	236	618	825	849	1,875	2,337
bbc-csm1-1	22	114	220	68	262	424	217	665	944	722	1,817	2,387
inmcm4	2	12	41	7	39	78	34	126	197	181	479	645
NASA	19	98	213	76	295	485	330	946	1,312	1,614	3,609	4,530

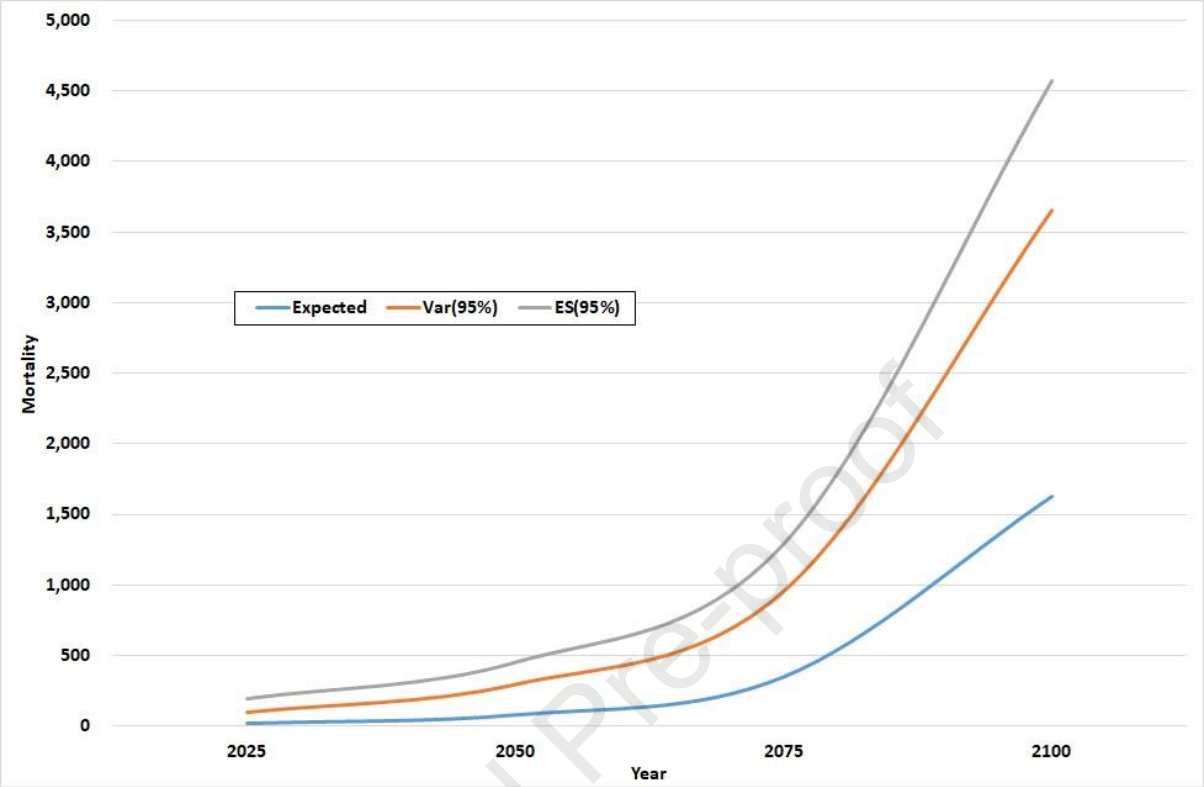

Fig. 5: Trend over time of mortality obtained with climate model 1 under RCP 8.5: Expected values, 95th percentile (Var(95%)) and Expected Shortfall (ES(95%)).

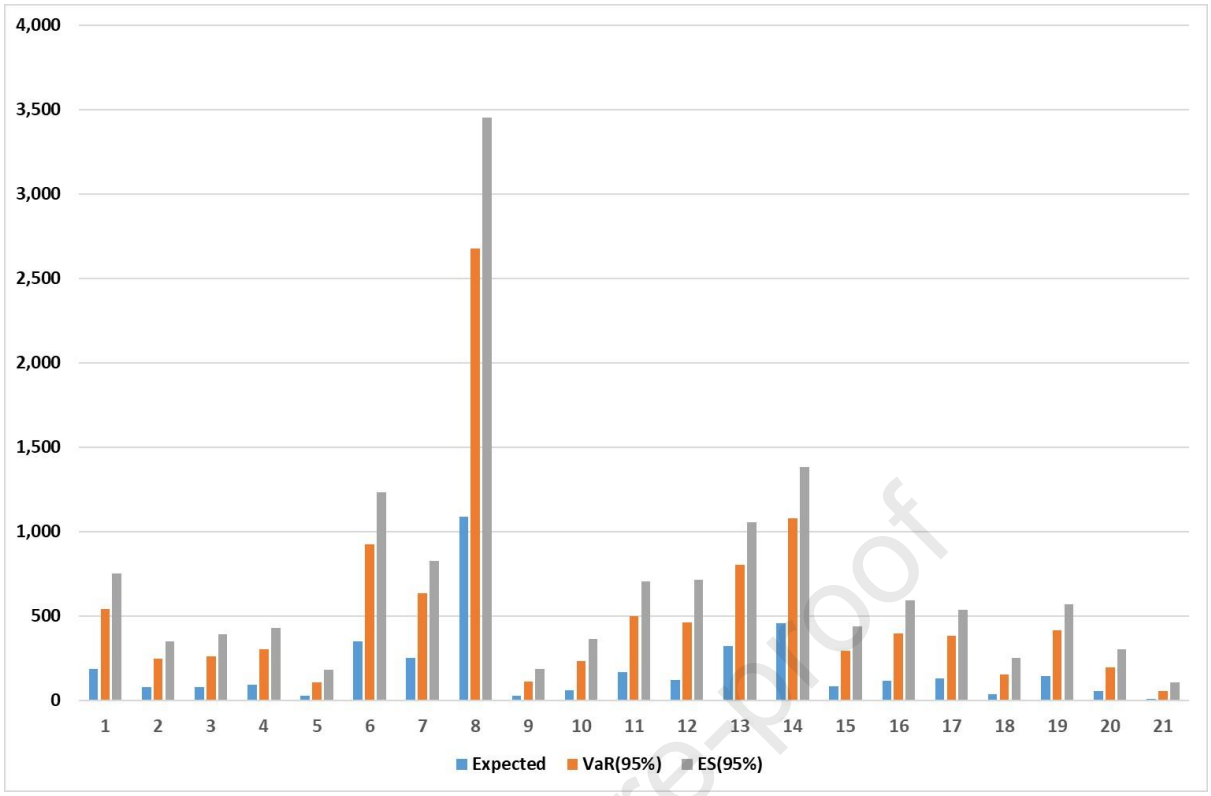

Fig. 6: Statistics for probabilistic mortality forecasts to 2100 (RCP 4.5) for the 21 climate models. Expected values, 95th percentile (VaR(95%)) and Expected Shortfall (ES(95%)).

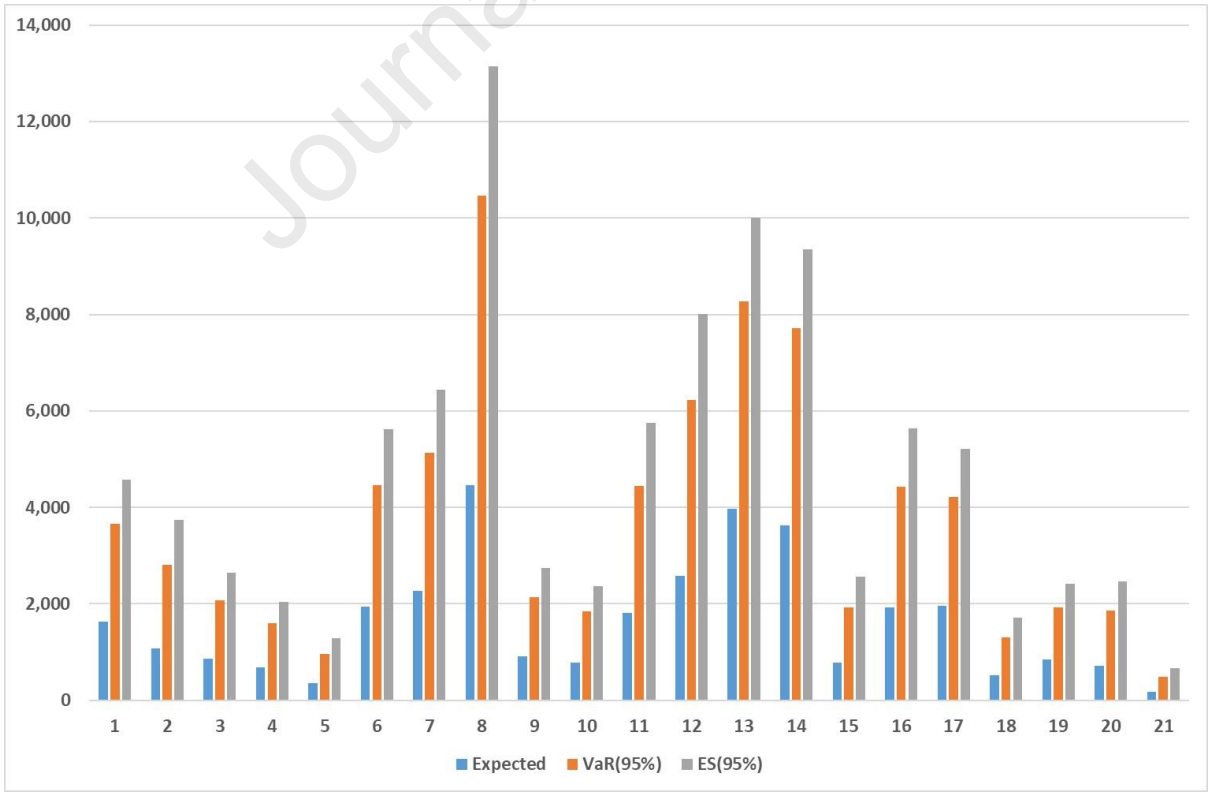

Fig. 7 Statistics for probabilistic mortality forecasts to 2100 (RCP 8.5) for the 21 models. Expected values, 95th percentile (Var(95%)) and Expected Shortfall (ES(95%)).

Figures 6 and 7 show significant differences in expected mortality and associated risk measures depending on the model selected for the RCP 4.5 and RCP 8.5 scenarios (see also Tables 6 and 7). Some scenarios generate extreme values and others moderate values. Tables 6 and 7 show the means of the risk values for the 21 climate models. Substantial differences between models can be seen. There is a distribution of results because there is a risk model problem.

3.4 Sensitivity analysis with potential acclimatisation

This section analyses potential acclimatisation, assuming that it is possible to acclimatise by absorbing the impact of half the expected excess temperature, as per proposed Equation (2), where there is a new maximum temperature T^*_{max} for each time *t*, that is:

$$T^*_{max} = T_{max} + \frac{temp(0) \times (e^{\beta t} - 1)}{2} \quad (2)$$

where β is as defined in Table 1.

The adaptation case involves the mean of model parameters in Table 8 and the mean of expected values in Table 9.

Table 8. Mean of model parameters in the adaptation case.

Parameters	RCP 4.5	RCP 8.5
λ(0)	1.568	1.705
α	0.012	0.018
dur(0)	1.277	1.083
γ	0.011	0.022
temp(0)	0.538	0.474
β	0.010	0.019
σ_E	0.592	0.585
$\rho_{1,2}$	0.437	0.371
$\rho_{2,3}$	0.636	0.539
σ_D	1.611	2.473

Table 9: Mean of expected values using the 21 climate models in the adaptation case.

Expected mean values	RCP 4.5	RCP 8.5
λ(t) 2025	1.96	2.32
λ(t) 2050	2.63	3.52
λ(t) 2075	3.57	5.42
λ(t) 2100	4.87	8.45
dur(t) 2025	1.57	1.64
dur(t) 2050	2.07	2.84
dur(t) 2075	2.75	5.00
dur(t) 2100	3.67	8.93
temp(t) 2025	0.64	0.67
temp(t) 2050	0.81	1.07
temp(t) 2075	1.04	1.73
temp(t) 2100	1.33	2.79

Tables 10 and 11 show the expected values and the risk measures in the adaptation case under the RCP 4.5 and RCP 8.5 scenarios respectively. For the same case, the figures also show major differences in duration and excess temperature depending on the model and scenario.

Table 12 shows significant differences between the models, risk metrics and acclimatisation. However, the differences between using a deterministic or stochastic MR are not significant.

Compared to Abadie et al. (2019), this paper makes four contributions: (1) it analyses the behaviour of 21 climate models for a city (Madrid); (2) it provides a stochastic modelling of the epidemiological counterpart; (3) it calculates adaptation effects (acclimatisation); (4) it corrects the statistical bias for the maximum temperatures for the city of Madrid; and (5) it calculates new epidemiological values for Madid city using data from 2010 to 2018. The statistical bias correction adjusts the future projections of each climate model to produce internally consistent fields that have the same statistical intensity distribution as climate observations (e.g., in this study climate observations from Madrid's El Retiro Park are used. These data sets are provided by the Spanish Meteorology Agency, AEMET) (Piani et al. 2010, Gudmundsson et al. 2012).

Table 10: Results for Madrid under the RCP 4.5 scenario, with adaptation.

	2025			2050			2075			2100		
	Expected	VaR(95%)	ES(95%)	Expected	VaR(95%)	ES(95%)	Expected	VaR(95%)	ES(95%)	Expected	VaR(95%)	ES(95%)
ACCESS1-0	13	63	115	28	113	186	62	214	316	136	402	562
BNU-ESM	13	63	115	16	67	115	30	109	172	55	179	261
CCSM4	16	74	129	25	106	173	40	151	239	63	223	329
CESM1(BGC)	11	53	99	19	84	145	36	137	217	65	222	325
CNRM-CM5	3	18	52	5	30	71	10	51	100	20	88	156
CSIRO-Mk3.6.0	18	84	155	43	167	270	106	351	515	267	754	1,022
CanESM2	17	73	122	38	135	201	81	245	347	172	463	620
GFDL-CM3	49	220	378	118	420	634	288	851	1,183	713	1,805	2,366
GFDL-ESM2G	11	55	103	15	69	120	20	87	147	26	110	177
GFDL-ESM2M	8	52	115	15	80	161	29	129	229	53	211	336
IPSL-CMSA-LR	3	24	64	10	55	109	32	131	215	105	336	484
IPSL-CM5A-MR	11	70	176	21	119	253	42	203	369	86	348	566
MIROC-ESM	16	70	116	39	138	208	94	278	388	227	585	773
MIROC-ESM-CHEM	27	102	159	60	194	281	136	373	511	313	761	993
MIROC5	10	54	105	19	89	157	36	146	241	68	244	378
MPI-ESM-LR	4	27	66	10	58	113	29	129	217	82	293	446
MPI-ESM-MR	5	29	67	12	58	109	31	119	189	81	257	369
MRI-CGCM3	2	15	55	4	29	78	10	57	119	26	114	201
NorESM1-M	16	70	119	30	111	175	55	180	261	99	290	400
bbc-csm1-1	5	32	79	10	54	109	20	93	166	42	161	258
inmcm4	1	7	28	2	14	40	4	25	57	8	47	92
NASA	12	60	115	26	104	177	57	193	295	129	376	529

Table 11: Results for Madrid under the RCP 8.5 scenario, with adaptation.

	2025			2050			2075			2100		
	Expected	VaR(95%)	ES(95%)	Expected	VaR(95%)	ES(95%)	Expected	VaR(95%)	ES(95%)	Expected	VaR(95%)	ES(95%)
ACCESS1-0	17	85	168	61	229	366	238	686	951	949	2,200	2,789
BNU-ESM	14	71	152	47	182	300	166	502	702	636	1,530	1,984
CCSM4	20	93	167	59	215	332	180	527	734	566	1,373	1,779
CESM1(BGC)	16	73	134	48	171	270	147	424	589	467	1,115	1,448
CNRM-CM5	1	13	40	8	45	92	40	156	247	213	606	836
CSIRO-Mk3.6.0	18	90	181	68	249	400	274	770	1,057	1,173	2,617	3,325
CanESM2	31	144	268	104	361	549	369	987	1,340	1,338	2,961	3,695
GFDL-CM3	55	261	449	193	664	970	671	1,813	2,408	2,396	5,464	6,827
GFDL-ESM2G	6	34	83	24	101	175	108	334	483	528	1,258	1,630
GFDL-ESM2M	12	71	148	40	171	288	142	452	659	499	1,279	1,690
IPSL-CMSA-LR	11	64	197	49	231	451	220	799	1,222	1,092	3,017	4,071
IPSL-CM5A-MR	17	92	233	59	264	466	235	765	1,109	1,038	2,559	3,359
MIROC-ESM	22	109	241	85	324	517	368	1,005	1,362	1,757	3,703	4,579
MIROC-ESM-CHEM	37	171	326	131	450	677	497	1,266	1,678	2,002	4,195	5,156
MIROC5	10	61	127	36	153	255	130	415	600	478	1,213	1,588
MPI-ESM-LR	11	63	171	44	194	341	214	655	928	1,167	2,688	3,431
MPI-ESM-MR	10	49	107	39	144	230	181	490	668	894	1,931	2,410
MRI-CGCM3	2	20	66	10	61	126	55	202	313	306	803	1,079
NorESM1-M	16	70	127	50	176	263	165	452	616	558	1,281	1,637
bbc-csm1-1	18	90	174	50	197	324	147	466	663	456	1,175	1,561
inmcm4	2	11	38	6	33	69	25	98	159	111	322	448
NASA	16	83	171	58	220	355	218	632	880	887	2,061	2,634

Table 12: Sensitivity of mortality forecasts to modelling choices.

Items	Sensitivity
RCP 8.5 Expected 2100 →ES(95%) 2100	2.5-3.5
RCP 8.5 ES(95%) 2025 → ES(95%) 2100	110-40
ES(95%) 2100 RCP 4.5→ ES(95%) 2100 RCP 8.5	4-15
MR deterministic →MR stochastic	1.02
RCP 8.5 No acclimatisation ES(95%)→ acclimatization ES(95%)	0.58

4 CONCLUSIONS

Daily time series of maximum future temperatures drawn from climate models can be used to analyse HW characteristics (number, duration and intensity) including trends over time. These variables have volatilities and correlations. With all these values it is possible to estimate distributions of excess temperature above a critical value, which in the city of Madrid was set at 38ºC. These distributions enable expected values to be obtained, along with risk measures such as the 95thpercentile (VaR(95%) and the mean of the 5% of worst cases (ES(95%)). For these calculations, two scenarios are considered: RCP 8.5 and RCP 4.5, which enable differential effects depending on the probability assigned to each scenario to be analysed.

The climate information obtained is combined with an epidemiological model, where the mortality risk (MR) is stochastic, and is modelled using a generalised extreme value distribution (gev). With these data the distributions of HW-related mortality are calculated for each time selected. The resulting distributions are then used to calculate expected values and risk measures. These risk measures are significant because the possible measures to be adopted should be suitable for counteracting the worst cases as far as possible and not just the expected average. Depending on the model selected ES(95%) may be between the two and six times the expected value.

Another source of risk is the climate model. When a climate model is selected, it assumed that the information which it generates is true. However, as proved in this paper, the downscaling information generated for each of the 21climate models selected is totally different and generates different expected and risk value measures for excess temperature and HW-related mortality. If a single climate model is used, depending on which model it is the results may be extreme compared to the average of all the climate models selected.

The mean under RCP 8.5 is an expected attributed mortality of 76 for 2050, increasing to 1,614 for 2100. The ES(95%) risk measure ranges from 494 in 2050 to 4,684 in 2100.

A possible acclimatisation effect is considered, assuming that it is possible to acclimatise by absorbing the impact of half the expected excess temperature. In that case the effects of HW-related mortality may be about 42% lower.

The proposed methodology can be applied to other cities, with a variety of results being obtained depending on each climate model. For this reason, this paper suggests the use of a set of climate models.

Appendix A.1. Determination of daily mortality threshold temperature and mortality risk.

In order to estimate the heat wave definition temperature (threshold or critical temperature) we follow to Diaz et al (2015) and Carmona et al. (2017). The procedure is described in the following lines:

1) we first fit an ARIMA model to the daily mortality due to natural causes for all days and for all the summer days (June, July, August and September; JJAS) for the period 2010-2018. The ARIMA fitting is estimated through the "auto.arima" function from the R package "forecast" that fits the best model taking into account the ACI/c and BIC criteria (Wang et al. 2006, Hyndman et al. 2008); 2) mortality residuals (i.e. the difference between the raw mortality and the fitted mortality) are used to estimate the mean value of the mortality and theirs corresponding confidence intervals (CI; 95%) for all days of the period 2010-2018 and for the summer days for the same period, these estimations are performed each 2ºC of the maximum daily temperature (Tmax) for the summers of the period 2010-2018; 3) a scatter-plot diagram is plotted by using the mean values of residuals mortality and their corresponding 95% CI (vertical axis) versus summer Tmax (each 2ºC) (horizontal axis) (Figure A.1).

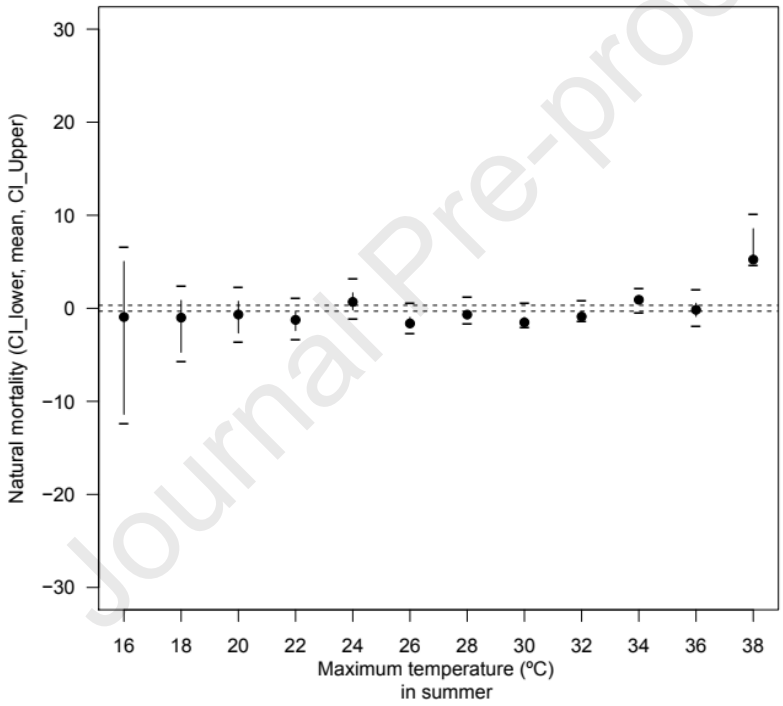

Figure A.1. Scatter plot for residuals of natural-cause mortality daily time series and daily maximum temperatures (ºC) for summer times for the period 2010-2018. The small black points correspond to the mean values of residuals of mortality and "-" are the 95% CI (lower and upper bounds). The horizontal dashed lines are the 95% CI for the mean value of residuals of mortality for all days of the period 2010-2018.

We have followed Díaz et al. (2015), Carmona et al. (2017) and López-Bueno et al. (2021) to estimate the RR and the MR. To estimate the RR we follow this procedure:

1) We fist calculated a new variable named Theat that is obtained as:

Theat = 0 if Tmax < Threshold
Theat = Tmax - Threshold if Tmax >= Threshold

where Tmax is the daily maximum temperatures for summer (from June to September; JJAS) and

Threshold is the daily mortality threshold temperature. The method used to estimate this threshold is based on Díaz et al (2015) and is explained previously in Appendix A.1.

2) We have fitted a Generalized Liner Model or GLM (using a Poisson family and a log link) between the new mortality rate (TM) as dependent variable and the Theat as independent variable. Furthermore, we have considered the short-term memory or persistence (lags from 1 to 4 days, where theirs corresponding variables are Theat1, Theat2, Theat3, and Theat4, respectively) of heat wave events on daily mortality following to Alberdi et al. (1998), Díaz et al. (2015) and Carmona et al. (2017). On the other hand, we have considered the trend and auto-correlation (coefficient at lag 1 and where its corresponding variable is TM1) as well as the seasonal components (yearly, six-monthly and quarterly) of the time series of mortality (Díaz et al. 2015, Carmona el at. 2017). This model is defined by the following formula (Carmona et al. 2017, López-Bueno et al. 2021):

Log(TM) = bo + b1 Trend + b2 sin(365) + b3 cos(365) + b4 sin(180) + b5 cos(180) + b6 sin(120) + b7 cos(120) + b8 sin(90) + b9 cos(90) + b10 TM1 + [b11 Theat + b12 Theat1 + b13 Theat2 + b14 Theat3 + b15 Theat4]

3) The heat-related relative risk (RR) is estimated as the e (2.7172) power of the sum of the coefficients b11, b12, b13, and b14 that are statistically significant (p-values < 0.05) (López-Bueno et al. 2021).

4). Finally, we have estimated the mortality risk (MR) (Díaz et al. 2015, Carmona el at. 2017), that is, MR = [(RR - 1)/RR]*100.

Appendix A.2. The stochastic HWs model.

There is assumed to be a Poisson process that generates HWs. The expected mean number of HWs at time *t* is estimated using Equation A.1:

$$\lambda(t) = \lambda(0)e^{\alpha t} \qquad \text{A.1}$$

The duration of an HW cannot be zero days, so there is also assumed to be a gamma process that determines the duration in days of an HW when it occurs. The expected mean duration of HWs at time *t* is estimated using Equation A.2:

$$d(t) = d(0)e^{\gamma t} \qquad \text{A.2}$$

In the gamma process their volatility is calibrated.

The temperature exceedance above 30ºC is obtained from a zero-truncated normal distribution correlated with the HW duration. The expected mean temperature exceedance over 38ºC at time *t* is estimated using Equation A.3:

$$g(t) = g(0)e^{\beta t} \quad \text{A.3}$$

Correlation between temperature exceedance and duration can be simulated by obtaining random samples correlated for temperature exceedance using Equation A.4:

$$\rho x_1 + x_2\sqrt{1-\rho^2} \quad \text{A.4}$$

where x_1 y x_2 are two independent, normalised samples of duration and temperature exceedance.

The Tables A.1 to A.2 show the parameters and expected values for Madrid under the RCP 4.5 and 8.5 respectively in the no adaptation case.

The Tables A.3 to A.4 show the parameters and expected values for Madrid under the RCP 4.5 and 8.5 respectively in the adaptation case.

Table A.1a: Parameters and expected values for Madrid under RCP 4.5, without adaptation.

	ACCESS1-0	BNU-ESM	CCSM4	CESM1(BGC)	CNRM-CM5	CSIRO-Mk3.6.0	CanESM2	GFDL-CM3	GFDL-ESM2G	GFDL-ESM2M	NASA
Parameters	M0145	M0245	M0345	M0445	M0545	M0645	M0745	M0845	M0945	M1045	Mean
λ(0)	1.392	1.504	1.678	1.569	0.768	1.815	2.523	3.371	1.856	1.468	1.621
α	0.015	0.011	0.011	0.012	0.013	0.015	0.011	0.009	0.006	0.012	0.013
dur(0)	1.768	1.492	1.839	1.506	0.724	1.488	1.689	2.205	1.283	1.114	1.309
γ	0.012	0.009	0.005	0.010	0.013	0.015	0.010	0.016	0.006	0.009	0.012
temp(0)	0.617	0.574	0.796	0.598	0.345	0.640	0.572	0.783	0.739	0.552	0.550
β	0.010	0.009	0.005	0.008	0.009	0.012	0.013	0.016	0.002	0.008	0.010
σ_E	0.546	0.565	0.638	0.540	0.562	0.558	0.467	0.720	0.599	0.692	0.595
$\rho_{1,2}$	0.315	0.227	0.430	0.252	0.662	0.446	0.423	0.280	0.540	0.610	0.430
$\rho_{2,3}$	0.585	0.305	0.628	0.614	0.806	0.718	0.709	0.716	0.678	0.796	0.645
σ_D	1.951	1.639	1.408	1.967	1.493	1.761	1.154	2.661	1.144	1.449	1.680
Expected	M0145	M0245	M0345	M0445	M0545	M0645	M0745	M0845	M0945	M1045	Mean
λ(t) 2025	1.86	1.86	2.08	1.95	0.98	2.43	3.14	4.03	2.10	1.84	2.06
λ(t) 2050	2.73	2.46	2.76	2.61	1.35	3.58	4.18	5.10	2.46	2.47	2.83
λ(t) 2075	4.01	3.24	3.67	3.48	1.85	5.27	5.56	6.45	2.89	3.33	3.93
λ(t) 2100	5.88	4.28	4.87	4.65	2.55	7.75	7.40	8.16	3.39	4.47	5.50
dur(t) 2025	2.21	1.78	2.01	1.81	0.93	1.96	2.05	3.00	1.43	1.32	1.63
dur(t) 2050	2.95	2.23	2.25	2.30	1.30	2.83	2.65	4.48	1.64	1.66	2.20
dur(t) 2075	3.95	2.81	2.53	2.94	1.81	4.08	3.41	6.71	1.89	2.08	2.99
dur(t) 2100	5.29	3.53	2.84	3.74	2.51	5.87	4.40	10.04	2.18	2.61	4.10
temp(t 2025	0.74	0.68	0.88	0.69	0.41	0.80	0.74	1.06	0.76	0.64	0.67
temp(t 2050	0.94	0.85	1.01	0.84	0.52	1.09	1.03	1.57	0.79	0.79	0.86
temp(t 2075	1.19	1.07	1.16	1.03	0.65	1.47	1.44	2.34	0.82	0.96	1.12
temp(t 2100	1.51	1.34	1.33	1.25	0.82	1.98	2.00	3.48	0.85	1.18	1.48

Table A.1b: Parameters and expected values for Madrid under RCP 4.5, without adaptation.

	IPSL-CMSA-LR	IPSL-CM5A-MR	MIROC-ESM	MIROC-ESM-CHEM	MIROC5	MPI-ESM-LR	MPI-ESM-MR	MRI-CGCM3	NorESM1-M	bbc-csm1-1	inmcm4	NASA
Parameters	M1145	M1245	M1345	M1445	M1545	M1645	M1745	M1845	M1945	M2045	M2145	Mean
λ(0)	0.961	1.064	2.783	3.342	1.484	0.723	1.107	0.745	2.517	1.006	0.369	1.621
α	0.016	0.014	0.015	0.013	0.015	0.024	0.017	0.014	0.007	0.011	0.020	0.013
dur(0)	1.051	1.774	1.243	1.323	1.363	1.172	0.705	0.621	1.620	1.070	0.436	1.309
γ	0.019	0.011	0.012	0.014	0.008	0.011	0.020	0.017	0.011	0.012	0.013	0.012
temp(0)	0.249	0.542	0.560	0.768	0.593	0.395	0.438	0.219	0.675	0.546	0.359	0.550
β	0.020	0.010	0.014	0.011	0.007	0.012	0.011	0.016	0.009	0.009	0.007	0.010
σ_E	0.527	0.772	0.484	0.510	0.621	0.601	0.532	0.587	0.562	0.695	0.724	0.595
$\rho_{1,2}$	0.377	0.292	0.517	0.302	0.530	0.446	0.492	0.730	0.011	0.444	0.701	0.430
$\rho_{2,3}$	0.624	0.653	0.649	0.505	0.732	0.771	0.629	0.806	0.516	0.498	0.604	0.645
σ_D	2.346	3.347	1.119	1.270	1.315	1.726	1.482	1.591	1.880	1.701	0.886	1.680
Expected	M1145	M1245	M1345	M1445	M1545	M1645	M1745	M1845	M1945	M2045	M2145	Mean
λ(t) 2025	1.30	1.38	3.67	4.26	1.99	1.15	1.52	0.98	2.89	1.24	0.53	2.06
λ(t) 2050	1.94	1.94	5.28	5.87	2.93	2.11	2.31	1.41	3.46	1.63	0.87	2.83
λ(t) 2075	2.90	2.74	7.59	8.09	4.31	3.87	3.52	2.02	4.14	2.14	1.42	3.93
λ(t) 2100	4.33	3.85	10.92	11.15	6.34	7.10	5.34	2.91	4.96	2.81	2.31	5.50
dur(t) 2025	1.50	2.21	1.56	1.73	1.58	1.44	1.04	0.85	1.99	1.35	0.56	1.63
dur(t) 2050	2.38	2.94	2.09	2.45	1.91	1.90	1.72	1.29	2.61	1.84	0.77	2.20
dur(t) 2075	3.79	3.92	2.81	3.48	2.31	2.50	2.87	1.94	3.42	2.51	1.06	2.99
dur(t) 2100	6.03	5.23	3.77	4.93	2.80	3.28	4.77	2.94	4.49	3.42	1.46	4.10
temp(t 2025	0.36	0.65	0.73	0.95	0.68	0.49	0.54	0.29	0.81	0.65	0.41	0.67
temp(t 2050	0.59	0.83	1.03	1.27	0.80	0.66	0.72	0.44	1.02	0.81	0.48	0.86
temp(t 2075	0.96	1.06	1.45	1.68	0.95	0.89	0.95	0.65	1.30	1.02	0.57	1.12
temp(t 2100	1.57	1.36	2.05	2.23	1.13	1.19	1.26	0.96	1.64	1.28	0.67	1.48

Table A.2a: parameters and expected values for Madrid under RCP 8.5, without adaptation.

	ACCESS1-0	BNU-ESM	CCSM4	CESM1(BGC)	CNRM-CM5	CSIRO-Mk3.6.0	CanESM2	GFDL-CM3	GFDL-ESM2G	GFDL-ESM2M	NASA
Parameters	M0185	M0245	M0385	M0485	M0585	M0685	M0785	M0885	M0985	M1085	Mean
λ(0)	1.906	1.375	2.143	1.574	0.317	1.996	3.036	3.763	1.069	1.994	1.966
α	0.016	0.019	0.016	0.019	0.036	0.017	0.009	0.006	0.025	0.017	0.017
dur(0)	1.178	1.330	1.398	1.617	0.766	1.186	1.634	1.923	0.770	1.094	1.038
γ	0.027	0.022	0.019	0.016	0.019	0.026	0.026	0.028	0.023	0.019	0.027
temp(0)	0.504	0.635	0.604	0.655	0.239	0.495	0.626	0.728	0.325	0.446	0.472
β	0.020	0.017	0.017	0.015	0.023	0.022	0.021	0.024	0.024	0.021	0.022
σ_E	0.559	0.694	0.543	0.571	0.572	0.500	0.563	0.735	0.592	0.695	0.593
$\rho_{1,2}$	0.203	0.180	0.252	0.388	0.551	0.327	0.115	-0.111	0.691	0.502	0.322
$\rho_{2,3}$	0.394	0.241	0.567	0.343	0.867	0.478	0.366	0.240	0.723	0.674	0.505
σ_D	3.053	4.756	2.343	1.728	1.619	3.611	4.341	8.719	1.541	1.538	3.262
Expected	M0185	M0245	M0385	M0485	M0585	M0685	M0785	M0885	M0985	M1085	Mean
λ(t) 2025	2.59	1.98	2.91	2.27	0.63	2.77	3.63	4.24	1.71	2.74	2.60
λ(t) 2050	3.89	3.20	4.34	3.66	1.56	4.27	4.59	4.96	3.16	4.17	3.82
λ(t) 2075	5.84	5.18	6.49	5.90	3.84	6.58	5.80	5.81	5.86	6.33	5.74
λ(t) 2100	8.77	8.38	9.69	9.53	9.48	10.14	7.33	6.80	10.86	9.62	8.82
dur(t) 2025	1.96	2.03	2.00	2.20	1.10	1.93	2.67	3.26	1.20	1.57	1.65
dur(t) 2050	3.84	3.52	3.22	3.31	1.77	3.66	5.11	6.55	2.14	2.52	3.11
dur(t) 2075	7.50	6.12	5.16	4.96	2.86	6.93	9.75	13.13	3.83	4.05	6.11
dur(t) 2100	14.67	10.64	8.28	7.45	4.61	13.14	18.64	26.34	6.84	6.50	12.69
temp(t 2025	0.74	0.88	0.83	0.87	0.37	0.75	0.93	1.15	0.52	0.67	0.70
temp(t 2050	1.24	1.36	1.26	1.25	0.65	1.31	1.58	2.08	0.95	1.13	1.20
temp(t 2075	2.07	2.10	1.92	1.81	1.16	2.27	2.66	3.78	1.76	1.93	2.06
temp(t 2100	3.45	3.25	2.92	2.61	2.05	3.93	4.50	6.86	3.24	3.28	3.56

Table A.2b: parameters and expected values for Madrid under RCP 8.5, without adaptation.

	IPSL-CMSA-LR	IPSL-CM5A-MR	MIROC-ESM	MIROC-ESM-CHEM	MIROC5	MPI-ESM-LR	MPI-ESM-MR	MRI-CGCM3	NorESM1-M	bbc-csm1-1	inmcm4	NASA
Parameters	M1185	M1285	M1385	M1485	M1585	M1685	M1785	M1885	M1985	M2085	M2185	Mean
λ(0)	1.049	1.700	3.868	4.110	1.824	2.284	1.896	1.039	2.189	1.619	0.543	1.966
α	0.023	0.016	0.010	0.008	0.019	0.014	0.016	0.021	0.015	0.016	0.027	0.017
dur(0)	1.445	0.221	0.224	0.933	0.965	0.727	0.531	0.515	1.294	1.626	0.415	1.038
γ	0.024	0.051	0.050	0.033	0.021	0.032	0.037	0.026	0.019	0.018	0.024	0.027
temp(0)	0.323	0.487	0.524	0.670	0.419	0.324	0.347	0.159	0.549	0.574	0.284	0.472
β	0.027	0.021	0.023	0.022	0.019	0.027	0.026	0.031	0.019	0.017	0.019	0.022
σ_E	0.609	0.668	0.495	0.510	0.637	0.584	0.484	0.644	0.519	0.622	0.646	0.593
$\rho_{1,2}$	0.400	0.066	0.049	0.088	0.406	0.277	0.226	0.706	0.444	0.316	0.681	0.322
$\rho_{2,3}$	0.592	0.418	0.427	0.513	0.658	0.551	0.134	0.834	0.497	0.644	0.441	0.505
σ_D	4.233	7.886	3.641	3.157	2.090	3.634	3.755	1.455	1.569	2.875	0.966	3.262
Expected	M1185	M1285	M1385	M1485	M1585	M1685	M1785	M1885	M1985	M2085	M2185	Mean
λ(t) 2025	1.61	2.31	4.64	4.83	2.64	2.99	2.57	1.56	2.91	2.20	0.91	2.60
λ(t) 2050	2.84	3.46	5.91	5.96	4.30	4.27	3.82	2.65	4.23	3.28	1.78	3.82
λ(t) 2075	5.00	5.18	7.51	7.37	7.00	6.10	5.69	4.51	6.15	4.91	3.49	5.74
λ(t) 2100	8.80	7.76	9.56	9.10	11.39	8.70	8.48	7.69	8.94	7.33	6.84	8.82
dur(t) 2025	2.28	0.58	0.58	1.74	1.43	1.34	1.06	0.84	1.85	2.31	0.65	1.65
dur(t) 2050	4.15	2.06	2.02	3.96	2.40	2.97	2.65	1.61	2.97	3.66	1.19	3.11
dur(t) 2075	7.57	7.31	7.03	9.00	4.02	6.62	6.60	3.09	4.75	5.80	2.17	6.11
dur(t) 2100	13.79	25.97	24.49	20.45	6.74	14.75	16.45	5.91	7.62	9.20	3.94	12.69
temp(t 2025	0.53	0.72	0.82	1.02	0.61	0.54	0.57	0.29	0.79	0.79	0.41	0.70
temp(t 2050	1.04	1.21	1.47	1.77	0.99	1.05	1.08	0.62	1.28	1.19	0.66	1.20
temp(t 2075	2.01	2.04	2.64	3.08	1.61	2.05	2.06	1.36	2.07	1.81	1.07	2.06
temp(t 2100	3.91	3.43	4.74	5.34	2.61	4.01	3.93	2.95	3.34	2.75	1.73	3.56

Table A.3a: Parameters and expected values for Madrid under RCP 4.5, with adaptation.

	ACCESS1-0	BNU-ESM	CCSM4	CESM1(BGC)	CNRM-CM5	CSIRO-Mk3.6.0	CanESM2	GFDL-CM3	GFDL-ESM2G	GFDL-ESM2M	NASA
Parameters	M0145	M0245	M0345	M0445	M0545	M0645	M0745	M0845	M0945	M1045	Mean
λ(0)	1.394	1.528	1.682	1.525	0.795	1.630	2.315	3.249	1.832	1.450	1.568
α	0.013	0.010	0.011	0.011	0.011	0.016	0.012	0.009	0.006	0.011	0.012
dur(0)	1.666	1.405	1.755	1.471	0.718	1.615	1.721	1.982	1.281	1.142	1.277
γ	0.012	0.008	0.005	0.008	0.012	0.012	0.008	0.016	0.006	0.009	0.011
temp(0)	0.612	0.560	0.794	0.607	0.320	0.626	0.541	0.779	0.739	0.518	0.538
β	0.009	0.008	0.005	0.007	0.010	0.011	0.012	0.014	0.001	0.008	0.010
σ_E	0.543	0.552	0.638	0.574	0.557	0.556	0.484	0.699	0.602	0.699	0.592
$\rho_{1,2}$	0.328	0.377	0.373	0.335	0.674	0.233	0.470	0.277	0.534	0.484	0.437
$\rho_{2,3}$	0.598	0.332	0.642	0.627	0.805	0.606	0.668	0.686	0.678	0.742	0.636
σ_D	1.762	1.289	1.384	1.467	1.442	2.181	1.144	2.523	1.155	1.629	1.611
Expected	M0145	M0245	M0345	M0445	M0545	M0645	M0745	M0845	M0945	M1045	Mean
λ(t) 2025	1.79	1.84	2.05	1.89	0.98	2.20	2.88	3.82	2.06	1.78	1.96
λ(t) 2050	2.48	2.34	2.67	2.52	1.29	3.27	3.85	4.74	2.41	2.34	2.63
λ(t) 2075	3.44	2.99	3.47	3.34	1.69	4.86	5.14	5.88	2.82	3.07	3.57
λ(t) 2100	4.78	3.81	4.51	4.44	2.22	7.22	6.86	7.29	3.30	4.03	4.87
dur(t) 2025	2.09	1.64	1.92	1.71	0.90	2.04	2.01	2.70	1.43	1.35	1.57
dur(t) 2050	2.82	2.02	2.16	2.09	1.23	2.76	2.46	4.04	1.65	1.67	2.07
dur(t) 2075	3.80	2.48	2.44	2.55	1.66	3.74	3.01	6.06	1.90	2.07	2.75
dur(t) 2100	5.13	3.05	2.74	3.12	2.25	5.08	3.69	9.08	2.19	2.57	3.67
temp(t 2025	0.72	0.65	0.87	0.69	0.39	0.78	0.68	1.01	0.76	0.61	0.64
temp(t 2050	0.90	0.80	0.97	0.82	0.50	1.03	0.93	1.42	0.78	0.75	0.81
temp(t 2075	1.12	0.98	1.09	0.96	0.63	1.38	1.27	1.99	0.81	0.93	1.04
temp(t 2100	1.40	1.20	1.22	1.14	0.81	1.83	1.73	2.79	0.83	1.14	1.33

Table A.3b: Parameters for Madrid under RCP 4.5, with adaptation.

	IPSL-CMSA-LR	IPSL-CM5A-MR	MIROC-ESM	MIROC-ESM-CHEM	MIROC5	MPI-ESM-LR	MPI-ESM-MR	MRI-CGCM3	NorESM1-M	bbc-csm1-1	inmcm4	NASA
Parameters	M114	M1245	M1345	M1445	M1545	M1645	M1745	M1845	M1945	M2045	M2145	Mean
λ(0)	0.873	1.154	2.615	3.214	1.438	0.713	1.035	0.713	2.400	0.975	0.394	1.568
α	0.015	0.010	0.014	0.012	0.014	0.022	0.016	0.014	0.006	0.011	0.018	0.012
dur(0)	0.944	1.638	1.201	1.298	1.387	1.099	0.824	0.642	1.515	1.080	0.440	1.277
γ	0.018	0.013	0.011	0.012	0.007	0.010	0.016	0.014	0.010	0.010	0.012	0.011
temp(0)	0.238	0.540	0.545	0.746	0.581	0.370	0.428	0.218	0.664	0.517	0.347	0.538
β	0.018	0.009	0.013	0.011	0.007	0.011	0.010	0.014	0.008	0.009	0.006	0.010
σ_E	0.520	0.759	0.462	0.495	0.621	0.581	0.523	0.585	0.533	0.734	0.706	0.592
$\rho_{1,2}$	0.428	0.251	0.483	0.397	0.534	0.452	0.628	0.662	0.169	0.389	0.689	0.437
$\rho_{2,3}$	0.694	0.609	0.631	0.553	0.707	0.800	0.650	0.776	0.477	0.488	0.594	0.636
σ_D	2.053	3.649	1.082	1.095	1.395	1.697	1.292	1.648	1.460	1.571	0.904	1.611
Expected	M114	M1245	M1345	M1445	M1545	M1645	M1745	M1845	M1945	M2045	M2145	Mean
λ(t) 2025	1.16	1.39	3.40	4.05	1.87	1.09	1.40	0.93	2.71	1.21	0.55	1.96
λ(t) 2050	1.70	1.77	4.79	5.50	2.65	1.92	2.09	1.30	3.18	1.60	0.85	2.63
λ(t) 2075	2.47	2.26	6.77	7.46	3.74	3.36	3.12	1.84	3.73	2.11	1.32	3.57
λ(t) 2100	3.61	2.89	9.55	10.11	5.29	5.89	4.66	2.59	4.38	2.79	2.06	4.87
dur(t) 2025	1.34	2.09	1.47	1.63	1.59	1.34	1.12	0.84	1.84	1.31	0.56	1.57
dur(t) 2050	2.12	2.86	1.93	2.21	1.91	1.74	1.68	1.21	2.38	1.70	0.76	2.07
dur(t) 2075	3.35	3.94	2.53	3.00	2.29	2.26	2.52	1.73	3.07	2.20	1.04	2.75
dur(t) 2100	5.30	5.41	3.32	4.06	2.75	2.93	3.79	2.49	3.97	2.84	1.42	3.67
temp(t 2025	0.34	0.64	0.70	0.91	0.66	0.46	0.52	0.29	0.78	0.62	0.39	0.64
temp(t 2050	0.53	0.80	0.96	1.19	0.78	0.61	0.67	0.41	0.96	0.77	0.45	0.81
temp(t 2075	0.84	1.00	1.33	1.55	0.92	0.81	0.87	0.58	1.19	0.97	0.52	1.04
temp(t 2100	1.34	1.25	1.84	2.03	1.08	1.08	1.13	0.82	1.47	1.22	0.60	1.33

Table A.4a: Parameters and expected values for Madrid under RCP 8.5, with adaptation.

	ACCESS1-0	BNU-ESM	CCSM4	CESM1(BGC)	CNRM-CM5	CSIRO-Mk3.6.0	CanESM2	GFDL-CM3	GFDL-ESM2G	GFDL-ESM2M	NASA
Parameters	M0185	M0245	M0385	M0485	M0585	M0685	M0785	M0885	M0985	M1085	Mean
λ(0)	1.579	1.238	1.775	1.473	0.378	1.880	2.707	3.242	0.901	1.647	1.705
α	0.019	0.019	0.017	0.018	0.032	0.018	0.012	0.008	0.025	0.018	0.018
dur(0)	1.343	1.155	1.419	1.422	0.726	1.111	1.499	1.991	0.751	1.107	1.083
γ	0.021	0.021	0.017	0.017	0.018	0.024	0.022	0.024	0.021	0.018	0.022
temp(0)	0.510	0.609	0.626	0.643	0.216	0.483	0.594	0.699	0.354	0.452	0.474
β	0.018	0.016	0.014	0.013	0.022	0.020	0.019	0.021	0.021	0.019	0.019
σ_E	0.556	0.657	0.554	0.572	0.553	0.512	0.553	0.702	0.598	0.688	0.585
$\rho_{1,2}$	0.236	0.418	0.275	0.354	0.491	0.314	0.240	-0.001	0.724	0.382	0.371
$\rho_{2,3}$	0.471	0.405	0.530	0.370	0.834	0.498	0.316	0.548	0.668	0.610	0.539
σ_D	2.731	2.202	2.172	1.833	1.665	2.657	3.048	4.352	1.341	1.911	2.473
Expected	M0185	M0245	M0385	M0485	M0585	M0685	M0785	M0885	M0985	M1085	Mean
λ(t) 2025	2.26	1.77	2.44	2.09	0.69	2.62	3.42	3.77	1.46	2.30	2.32
λ(t) 2050	3.64	2.83	3.71	3.30	1.53	4.07	4.65	4.61	2.75	3.58	3.52
λ(t) 2075	5.86	4.53	5.63	5.21	3.40	6.32	6.32	5.63	5.17	5.57	5.42
λ(t) 2100	9.41	7.25	8.55	8.24	7.54	9.80	8.59	6.87	9.74	8.65	8.45
dur(t) 2025	2.00	1.73	1.97	1.97	1.03	1.75	2.30	3.12	1.13	1.55	1.64
dur(t) 2050	3.39	2.95	3.03	3.02	1.63	3.18	4.03	5.64	1.92	2.40	2.84
dur(t) 2075	5.75	5.02	4.67	4.63	2.59	5.78	7.06	10.20	3.27	3.72	5.00
dur(t) 2100	9.73	8.55	7.19	7.10	4.11	10.51	12.37	18.44	5.56	5.76	8.93
temp(t 2025	0.72	0.82	0.82	0.82	0.33	0.70	0.85	1.05	0.53	0.64	0.67
temp(t 2050	1.13	1.23	1.18	1.13	0.57	1.14	1.35	1.77	0.89	1.02	1.07
temp(t 2075	1.76	1.83	1.69	1.56	0.98	1.87	2.15	3.01	1.50	1.62	1.73
temp(t 2100	2.77	2.72	2.43	2.15	1.68	3.05	3.42	5.10	2.54	2.58	2.79

Table A.4b: Parameters and expected values for Madrid under RCP 8.5, with adaptation.

	IPSL-CMSA-LR	IPSL-CM5A-MR	MIROC-ESM	MIROC-ESM-CHEM	MIROC5	MPI-ESM-LR	MPI-ESM-MR	MRI-CGCM3	NorESM1-M	bbc-csm1-1	inmcm4	NASA
Parameters	M1185	M1285	M1385	M1485	M1585	M1685	M1785	M1885	M1985	M2085	M2185	Mean
λ(0)	0.788	1.468	3.154	3.794	1.553	2.007	1.553	0.920	1.777	1.471	0.493	1.705
α	0.024	0.018	0.015	0.011	0.020	0.016	0.019	0.020	0.017	0.017	0.025	0.018
dur(0)	1.713	0.931	0.611	0.949	1.010	0.521	0.852	0.465	1.268	1.462	0.424	1.083
γ	0.020	0.028	0.031	0.028	0.018	0.033	0.025	0.026	0.017	0.017	0.023	0.022
temp(0)	0.309	0.519	0.537	0.688	0.409	0.344	0.358	0.173	0.547	0.584	0.291	0.474
β	0.025	0.017	0.020	0.018	0.018	0.023	0.023	0.027	0.017	0.015	0.018	0.019
σ_E	0.587	0.679	0.483	0.509	0.611	0.568	0.494	0.607	0.506	0.646	0.645	0.585
$\rho_{1,2}$	0.292	0.222	0.282	0.177	0.430	0.288	0.484	0.631	0.391	0.452	0.708	0.371
$\rho_{2,3}$	0.445	0.554	0.449	0.377	0.747	0.599	0.412	0.843	0.495	0.648	0.505	0.539
σ_D	6.012	4.007	2.534	2.872	1.756	2.812	1.696	1.572	1.605	2.139	1.019	2.473
Expected	M1185	M1285	M1385	M1485	M1585	M1685	M1785	M1885	M1985	M2085	M2185	Mean
λ(t) 2025	1.25	2.05	4.16	4.68	2.27	2.70	2.21	1.35	2.43	2.02	0.79	2.32
λ(t) 2050	2.30	3.19	6.00	6.16	3.73	3.99	3.52	2.22	3.68	3.06	1.46	3.52
λ(t) 2075	4.23	4.96	8.64	8.11	6.13	5.90	5.61	3.67	5.56	4.65	2.72	5.42
λ(t) 2100	7.78	7.71	12.45	10.67	10.07	8.71	8.93	6.06	8.41	7.06	5.04	8.45
dur(t) 2025	2.51	1.60	1.09	1.62	1.42	0.98	1.37	0.77	1.77	2.00	0.66	1.64
dur(t) 2050	4.16	3.26	2.36	3.26	2.22	2.26	2.58	1.48	2.73	3.04	1.16	2.84
dur(t) 2075	6.88	6.63	5.07	6.59	3.47	5.21	4.83	2.85	4.23	4.60	2.06	5.00
dur(t) 2100	11.39	13.50	10.92	13.28	5.42	11.99	9.07	5.51	6.54	6.97	3.65	8.93
temp(t 2025	0.49	0.72	0.78	0.98	0.58	0.53	0.55	0.29	0.76	0.77	0.41	0.67
temp(t 2050	0.91	1.11	1.29	1.55	0.91	0.94	0.97	0.58	1.16	1.12	0.63	1.07
temp(t 2075	1.68	1.70	2.13	2.45	1.43	1.67	1.71	1.15	1.77	1.63	0.98	1.73
temp(t 2100	3.12	2.61	3.51	3.88	2.25	2.96	3.00	2.29	2.70	2.36	1.52	2.79

Appendix A.3. The stochastic mortality risk model

The mortality risk (MR) is modelled as a generalised extreme value distribution (gev) whose cumulative distribution function is given by Equation (A.5).

$$F(x) = e^{(-(1+\xi\frac{x-\mu}{\sigma})^{-\frac{1}{\xi}})}, 1 + \xi\frac{x-\mu}{\sigma} > 0. \quad \text{(A.5)}$$

with three parameters:

$\mu \in R$ location, $\sigma > 0$ scale, $\xi \in R$ shape.

The probability density function (p.d.f.) is described by Equation (A.6) and (A.7):

$$\frac{1}{\sigma}(1 + \xi\frac{x-\mu}{\sigma})^{-\frac{\xi+1}{\xi}} e^{(-(1+\xi\frac{x-\mu}{\sigma})^{-\frac{1}{\xi}})}, \xi \neq 0 \quad \text{(A.6)}$$

$$e^{-\frac{x-\mu}{\sigma}}, \xi = 0. \quad \text{(A.7)}$$

The mean is calculated with Equations (A.8), (A.9) and (A.10)

$$\mu + \sigma(\Gamma(1-\xi) - 1), \text{if } \xi \neq 0, \xi < 1 \quad \text{(A.8)}$$

$$\mu + \sigma\gamma, \text{if } \xi \neq 0, \xi < 1 \quad \text{(A.9)}$$

$$\infty, \text{if } \xi \geq 1 \quad \text{(A.10)}$$

where Γ is the gamma funtion and γ is Euler´s constant ($\gamma = 0.5772$).

Figure A.1 shows the probability density function of the GEV distribution with the parameter values calculated.

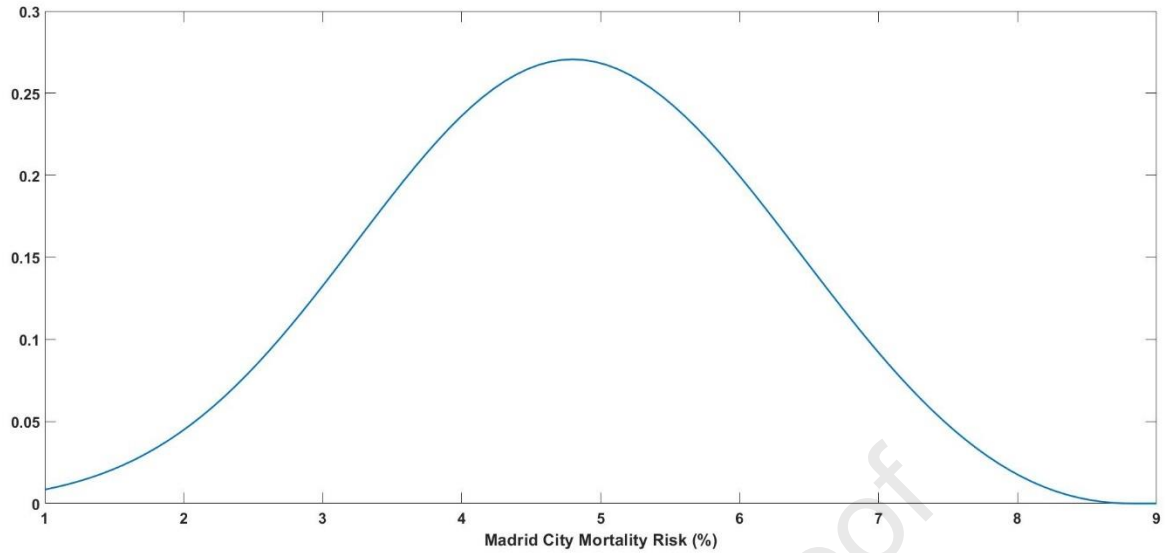

Fig. A.3. Probability density function GEV distribution.

Acknowledgements

This research is supported by the Basque Government through the BERC 2018-2021 programme and by the Spanish Ministry of Economy and Competitiveness (MINECO) through BC3 María de Maeztu excellence accreditation MDM-2017-0714. JMPM acknowledges funding support from the SEPE (Spanish National Employment Service), the Junta de Castilla y León, and the European Regional Development Fund (Grant CLU-2019-03). We would like to thank Dr. Marc Neumann for his helpful comments. The authors acknowledge to the Spanish Statistical Office - INE (petition: PB206/2021-REGI29396) for proving data of natural daily mortality for the period 2010-2018.

REFERENCES

Abadie, L. M., Chiabai, A., & Neumann N. B. (2019). Stochastic diffusion models to describe the evolution of annual HW statistics: A three-factor model with risk calculations, Science of the Total Environment, 646, 670-684. https://doi.org/10.1016/j.scitotenv.2018.07.158

Alberdi, J. C., Díaz, J., Montero, J. C., & Mirón, I. (1998). Daily mortality in Madrid community 1986–1992: relationship with meteorological variables. European Journal of Epidemiology, 14(6),

AEMET (2021) AEMET Open Data. www.opendata.aemet.es (last access July 8, 2021).

AghaKouchak, A., Chiang, F., Huning, L. S., Love, C.A., Mallakpour, I., Mazdiyasni, O., Moftakhari, H., Papalexiou, S.M., Ragno, E., & Sadegh, M. (2020). Climate extremes and compound hazards in a warming world. Annual Review of Earth and Planetary Sciences, 48, 519-548. https://doi.org/10.1146/annurev-earth-071719-055228

Allen, C. D., Macalady, A. K., Chenchouni, H., Bachelet, D., McDowell, N., Vennetier, M., ... & Cobb, N. (2010). A global overview of drought and heat-induced tree mortality reveals emerging climate change risks for forests. Forest Ecology Management, 259, 660–684. https://doi.org/10.1016/j.foreco.2009.09.001

Basu, R., & Samet, J. M. (2002). Relation between elevated ambient temperature and mortality: a review of the epidemiologic evidence. Epidemiologic Reviews, 24(2), 190-202. https://doi.org/10.1093/epirev/mxf007

Beniston, M. (2004). The 2003 heat wave in Europe: A shape of things to come? An analysis based on Swiss climatological data and model simulations. Geophysical Research Letters, 31(2), L02202. https://doi.org/10.1029/2003GL018857

Brown, S. J, Caesar J., & Ferro C. A. T. (2008). Global changes in extreme daily temperature since 1950. Journal of Geophysical Research, 113, D05115. https://doi.org/10.1029/2006JD008091

Campbell, S., Remenyi, T. A., White, C. J., & Johnston, F. H. (2018). Heatwave and health impact research: A global review. Health & Place, 53, 210-218. https://doi.org/10.1016/j.healthplace.2018.08.017

Carmona, R., Linares, C., Ortiz, C., Mirón, I. J., Luna, M. Y., & Díaz, J. (2017). Spatial variability in threshold temperatures of heat wave mortality: impact assessment on prevention plans. International Journal of Environmental Health Research, 27(6), 463-475. https://doi.org/10.1080/09603123.2017.1379056

Chapman, S. C., Watkins, N. W., & Stainforth, D. A. (2019). Warming Trends in Summer Heatwaves. Geophysical Research Letters, 46, 1634–1640. https://doi.org/10.1029/2018GL08100

Coles, S. G., Tawn, J. A., & Smith, R.L. (1994). A seasonal Markov model for extremely low temperatures. Environmetrics, 5, 221–239. https://doi.org/10.1002/env.3170050304

Díaz, J., Carmona, R., Mirón, I. J., Ortiz, C., León, I., & Linares, C. (2015). Geographical variation in relative risks associated with heat: Update of Spain's Heat Wave Prevention Plan. Environment International, 85, 273-283. https://doi:10.1016/j.envint.2015.09.022

Díaz, J., Sáez, M., Carmona, R., Mirón, I.J., Barceló, M.A., Luna, M. Y., & Linares, C. (2019) Mortality attributable to high temperatures over the 2021–2050 and 2051–2100 time horizons in Spain: Adaptation and economic estimate. Environmental Research, 172, 475-485. https://doi.org/10.1016/j.envres.2019.02.041

Fischer, E. M., & Schär, C. (2010). Consistent geographical patterns of changes in high-impact European heatwaves. Nature Geoscience, 3(6), 398-403. https://doi.org/10.1038/ngeo866

Follos, F., Linares, C., Vellón, J. M., Lopez-Bueno, J. A., Luna, M. Y., Sánchez-Martínez, G., & Díaz, J. (2020). The evolution of minimum mortality temperatures as an indicator of heat adaptation: The cases of Madrid and Seville (Spain). Science of The Total Environment, 747, 141259. https://doi.org/10.1016/j.scitotenv.2020.141259

Furrer, E. M., Katz R. W., Walter, M. D, & Furrer, R. (2010). Statistical modelling of hot spells and heat waves. Climate Research, 43, 191-205. https://doi.org/10.3354/cr00924

García-Herrera, R., Díaz, J., Trigo, R. M., Luterbacher, J., & Fischer, E. M. (2010). A review of the European summer heat wave of 2003. Critical Reviews in Environmental Science and Technology, 40(4), 267-306. https://doi.org/10.1080/10643380802238137

Gudmundsson, L., Bremnes, J. B., Haugen, J. E., & Engen-Skaugen, T. (2012). Technical Note: Downscaling RCM precipitation to station scale using statistical transformation – a comparison methods. Hydrology and Earth System Sciences, 16, 3383-3390. https://doi.org/10.5194/hess-16-3383-2012

He, C., Ma, L., Zhou, L., Kan, H., Zhang, Y., Ma, W., & Chen, B. (2019). Exploring the mechanisms of heat wave vulnerability at the urban scale based on the application of big data and artificial societies. Environment International, 127, 573-583. https://doi.org/10.1016/j.envint.2019.01.057

Hereş, A. M., Petritan, I. C., Bigler, C., Curtu, A. L., Petrea, Ş., Petritan, A. M., Polanco-Martínez, J. M., Rigling, A., & Yuste, J. C. (2021). Legacies of past forest management determine current responses to severe drought events of conifer species in the Romanian Carpathians. Science of The Total Environment, 751, 141851. https://doi.org/10.1016/j.scitotenv.2020.141851

Hyndman, R.J., & Khandakar, Y. (2008). Automatic time series forecasting: The forecast package for R. Journal of Statistical Software 27(1), 1-22. http://dx.doi.org/10.18637/jss.v027.i03

INE (2021) www.ine.es (last access July 23, 2021).

Kharin, V. V., Zwiers, F. W., Zhang, X., & Hegerl, G. C. (2007). Changes in temperature and precipitation extremes in the IPCC ensemble of global coupled model simulations. Journal of Climate, 20(8), 1419–1444. https://doi.org/10.1175/JCLI4066.1

Kyselý, J. (2010). Recent severe heatwaves in central Europe: how to view them in a long-term prospect?. International Journal of Climatology, 30, 89-109. https://doi.org/10.1002/joc.1874

López-Bueno, J. A., Navas-Martín, M. A., Linares, C., Mirón, I. J., Luna, M. Y., Sánchez-Martínez, G., ... & Díaz, J. (2021). Analysis of the impact of heat waves on daily mortality in urban and rural areas in Madrid. Environmental Research, 195, 10892. https://doi.org/10.1016/j.envres.2021.110892

López-Bueno, J. A., Díaz, J., Sánchez-Guevara, C., Sánchez-Martínez, G., Franco, M., Gullón, P., ... & Linares, C. (2020). The impact of heat waves on daily mortality in districts in Madrid: The effect of sociodemographic factors. Environmental Research, 190, 109993. https://doi.org/10.1016/j.envres.2020.109993

Macchiato, M, Serio, C., Lapenna V., &LaRotonda L. (1993). Parametric time series analysis of cold and hot spells in daily temperature: an application in southern Italy. Journal of Applied Meteorology, 32, 1270-1281. https://doi.org/10.1175/1520-0450(1993)032<1270:PTSAOC>2.0.CO;2

Mazdiyasni, O., AghaKouchak, A., Davis, S. J. ,Madadgar, S., Mehran, A., Ragno, E., Sadegh, M., Sengupta, A., Ghosh, S., Dhanya, C. T., & Niknejad, M. (2017). Increasing probability of mortality during Indian heat waves. Science Advances, 3, e1700066. https://doi.org/10.1126/sciadv.1700066

McGregor, G. R., Bessemoulin, P., Ebi, K.L., & Menne, B. (2015). Heatwaves and health: guidance on warning-system development. World Meteorological Organization and World Health Organization, http://www.who.int/globalchange/publications/WMO_WHO_Heat_Health_Guidance_2015.pdf

Meehl, G. A., & Tebaldi, C. (2004). More intense, more frequent, and longer lasting heat waves in the 21st century. Science, 305(5686), 994-997. https://doi.org/10.1126/science.1098704

Patz, J. A., Campbell-Lendrum, D., Holloway, T., & Foley, J. A. (2005). Impact of regional climate change on human health. Nature, 438(7066), 310-317. https://doi.org/10.1038/nature04188

Perkins, S. E., & Alexander, L. V. (2013). On the measurement of heat waves. Journal of Climate, 26(13), 4500-4517. https://doi.org/10.1175/JCLI-D-12-00383.1

Perkins-Kirkpatrick, S. E., & Lewis, S. C. (2020). Increasing trends in regional heatwaves. Nature Communications, 11, 3357. https://doi.org/10.1038/s41467-020-16970-7

Piani, C., Weedon, G. P., Best, M., Gomes, S. M., Viterbo, P., Hagemann, S., & Haerter, J. O. (2010). Statistical bias correction of global simulated daily precipitation and temperature for the application of

hydrological models. Journal of Hydrology, 395(3-4), 199-215. https://doi.org/10.1016/j.jhydrol.2010.10.024

Robine, J. M., Cheung, S. L. K., Le Roy, S., Van Oyen, H., Griffiths, C., Michel, J. P., & Herrmann, F. R. (2008). Death toll exceeded 70,000 in Europe during the summer of 2003. Comptes Rendus Biologies, 331(2), 171-178. . https://doi.org/10.1016/j.crvi.2007.12.001

Robinson, P. J. (2001). On the definition of a heat wave. Journal of Applied Meteorology and Climatology, 40(4), 762-775. https://doi.org/10.1175/1520-0450(2001)040<0762:OTDOAH>2.0.CO;2

Schär, C., Vidale, P. L., Lüthi, D., Frei, C., Häberli, C., Liniger, M. A., & Appenzeller, C. (2004). The role of increasing temperature variability in European summer heatwaves. Nature, 427(6972), 332-336. https://doi.org/10.1038/nature02300

Smith, M. D. (2011). An ecological perspective on extreme climatic events: a synthetic definition and framework to guide future research. Journal of Ecology, 99(3), 656-663. https://doi.org/10.1111/j.1365-2745.2011.01798.x

Tomlinson, C. J., Chapman, L., Thornes, J. E., & Baker, C. J. (2011). Including the urban heat island in spatial heat health risk assessment strategies: a case study for Birmingham, UK. International Journal of Health Geographics, 10(1), 1-14. https://doi.org/10.1186/1476-072X-10-42

Thrasher, B., Maurer, E. P., McKellar, C., & Duffy, P. B. (2012). Technical Note: Bias correcting climate model simulated daily temperature extremes with quantile mapping. Hydrology and Earth System Sciences, 16, 3309-3314. https://doi.org/10.5194/hess-16-3309-2012

Vautard, R., Gobiet, A., Jacob, D., Belda, M., Colette, A., Déqué, M., Fernández, J., García-Díez, M., Goergen, K., Güttler, I., & Halenka, T. (2013). The simulation of European heat waves from an ensemble of regional climate models within the EURO-CORDEX project. Climate Dynamics, 41(9-10), 2555-2575. https://doi.org/10.1007/s00382-013-1714-z

Wallemacq, P. (2018). Economic losses, poverty & disasters: 1998-2017. Centre for Research on the Epidemiology of Disasters, CRED, UNISDR.

Wang, X, Smith, KA, & Hyndman, R.J. (2006). Characteristic-based clustering for time series data. Data Mining and Knowledge Discovery, 13(3), 335-364.

WHO 2020: https://www.who.int/health-topics/heatwaves#tab=tab_1 (last accessed July 9, 2021)

Xu, Z., FitzGerald, G., Guo, Y., Jalaludin, B., & Tong, S. (2016). Impact of heatwave on mortality under different heatwave definitions: a systematic review and meta-analysis. Environment International, 89, 193-203. https://doi.org/10.1016/j.envint.2016.02.007

Declaration of interests

X The authors declare that they have no known competing financial interests or personal relationships that could have appeared to influence the work reported in this paper.

☐The authors declare the following financial interests/personal relationships which may be considered as potential competing interests:

.